Theses and Dissertations   Graduate School

2017

Evaluation of Volumetric Change of Periapical Lesions After Apicoectomy as a Measure of Postsurgical Healing Utilizing Cone Beam Computed Tomography

Eshwar Arasu
Virginia Commonwealth University

Evaluation of volumetric change of periapical lesions after apicoectomy as a measure of postsurgical healing utilizing cone beam computed tomography

A thesis submitted in partial fulfillment of the requirements for the degree of Master of Science in Dentistry at Virginia Commonwealth University

by

Eshwar Arasu
DMD, Harvard University, 2015
BSE in Biomedical Engineering, University of Michigan, 2011

Director: Dr. Garry L. Myers, DDS
Program Director, Advanced Education Program in Endodontics

Virginia Commonwealth University
Richmond, Virginia
May 2017

Table of Contents

List of Tables

List of Figures

Abstract

EVALUATION OF VOLUMETRIC CHANGE OF PERIAPICAL LESIONS AFTER
APICOECTOMY AS A MEASURE OF POSTSURGICAL HEALING UTILIZING CONE
BEAM COMPUTED TOMOGRAPHY

By Eshwar Arasu, DMD

A thesis submitted in partial fulfillment of the requirements for the degree of Master of Science
in Dentistry at Virginia Commonwealth University.

Virginia Commonwealth University, 2017

Director: Dr. Garry Myers, DDS
Program Director, Advanced Education Program in Endodontics

The aim of this study was to evaluate whether volumetric changes in persistent periapical lesions

can be detected in follow-ups six months to five years after apicoectomy using cone-beam

computed tomography. Patients with a previous treatment history of apicoectomy and for whom

a pre-surgical CBCT scan was taken between November 2010 and December 2015 were invited

to participate in the study. A post-surgical CBCT image of the treated tooth was obtained at the

recall visit. Volumetric and linear measurements of periapical lesions on initial and post-

operative CBCT images were performed using DiThreshGUI software and two calibrated

examiners—a board-certified endodontist and a board-certified oral radiologist. Repeated-

measures ANOVA were used to estimate the magnitude of reduction and to test for differences

(at alpha=0.05). A total of 20 patients with 27 surgically treated teeth were recalled at an average

interval of 37 months. Reduction in the size of lesions was observed in 24 teeth (88%); overall,

the volumes significantly decreased as detected by software-assisted measurement of volume (P

= .0002) and by calculation from linear measurements (P < .0001). Volumetric analysis detected a reduction of 86% in lesions while the linear-derived volume measurements yielded an average reduction of 96%. These two methods of lesion assessment were strongly correlated with one another in pre-surgical scans (r>0.88) when apical lesions are measurable.

Introduction

The prevention or elimination of apical periodontitis—an inflammation-mediated disease at the root end of teeth—is a major goal of endodontic therapy. Epidemiologic studies suggest that apical periodontitis is a common clinical problem and one that has been documented in nearly half of patients by age 50 (1). The immune-mediated inflammatory response to the infiltration of microorganisms and microbial byproducts in the pulp space of root canals has been shown to induce pathological changes at the apices of teeth, leading to apical periodontitis and the potential development of several types of periapical lesions (2, 3). Clinical resolution of these lesions is expected with successful endodontic intervention (4).

Nonsurgical endodontic therapy is often the primary treatment modality of apical periodontitis when the tooth has been deemed restorable, but an apicoectomy—also known as periapical microsurgery—may be indicated when periradicular pathosis is refractory to nonsurgical procedures (5). The histological status of a periapical lesion is unknown to clinicians who have historically relied on periapical radiography to diagnose apical periodontitis (6). While periapical granulomas tend to resolve after nonsurgical endodontic therapy, true periapical cysts—comprising approximately 10 percent of all periapical lesions—may require surgical intervention (6). Other indications to surgery are those factors that may predispose nonsurgically treated teeth to failure, which include apical transportation, instrument separation, and complex root canal anatomy (7).

The apicoectomy surgical protocol typically involves the administration of local anesthesia, reflection of a mucoperiosteal flap, osteotomization to reveal dental root apices, resection of the apices, retropreparation of the root canal space followed by a biocompatible root-end filling, and flap closure via sutures (7). The advent of microinstruments and microscopes for magnification and illumination have conferred clinicians the advantages of easier root apex identification, shallower resection angles, and more conservative coaxial root-end preparations (8). If performed with modern techniques, apicoectomies are associated with predictable outcomes with one recent systematic review reporting 89 percent success among patients undergoing the surgical procedure (9).

Several studies have investigated prognostic factors associated with endodontic surgical outcomes. The size of the pre-operative periapical lesion has been evaluated as one such factor; it has been proposed that large lesions are less likely to heal than smaller ones due to fibroblastic proliferation from the periosteum into the osseous defect, resulting in scar formation rather than bony fill (10). Some studies have reported improved outcomes in both traditional and modern endodontic surgery with smaller lesions—albeit without statistical significant difference (11-13). However, in contradiction, other studies have reported no significant correlation between procedural outcome and size of pre-operative lesion in both traditional and modern apical surgeries (14, 15).

Periapical radiography has traditionally been utilized to evaluate the size of periapical lesions, but this imaging technology is limited by its capacity to render clinical information in only two dimensions. More specifically, the bucco-lingual dimension cannot be determined with radiographs. Superimposition of adjacent anatomic structures, such as the zygomatic process and maxillary sinus, also complicate accurate interpretation of radiographs. Moreover, periapical

rarefaction can only be visualized in a radiograph when the bone has been demineralized by about 30 to 50 percent (16).

Cone-beam computed tomography (CBCT) is a modern three-dimensional radiographic imaging technique that is instrumental to pre-surgical assessment, particularly for its capacity to resolve the anatomic proximity of root apices to other structures such as the inferior alveolar canal, mental foramen, and maxillary sinus (17-19). CBCT imaging facilitates the visualization of periapical lesions that are of small size and confined within cancellous bone, which are often imperceptible on periapical radiographs (20, 21). Moreover, CBCT-resolved lesions can be assessed in all three orthogonal planes for accurate dimensional measurement and volumetric analysis (22). Studies that have pitted the diagnostic capacities of periapical radiography against CBCT have reported that the latter modality enabled clinicians to identify more periapical lesions both *in vitro* and *in vivo* (20, 23, 24).

The use of CBCT is not only valuable in pre-surgical planning but also may be deployed post-surgically in the assessment of healing. In a 2016 study of 61 surgically treated roots, Von Arx et al. devised criteria for three-dimensional outcome assessment of apical surgery (25). In the study, radiographic healing was examined and indices assigned at the resection plane, within the apical area, at the cortical plate. A combined assessment of apical and cortical defects in the buccolingual plane, which was termed the B index, was found to be highly reproducible between observers and was consequently recommended for use in future studies of radiographic surgical outcome assessment.

Several studies in periodontic, orthodontic, and maxillofacial surgical literature have relied on quantitative measurements within CBCT imaging for research methodology, but only recently have they been gaining a foothold in endodontics. One study reported a high correlation

($R^2 = 94.6 – 99.3\%$) between direct caliper and CBCT-assisted linear measurements of simulated periapical lesions (26). Liang et al. (27) reported high accuracy of volumetric assessment with CBCT when compared against physical silicone replica molds taken of artificial periapical lesions. At present, CBCT-assisted volumetric analysis can be achieved with high accuracy using a variety of software platforms (28, 29).

CBCT studies of volumetric changes in periapical lesions have been conducted either in the context of pre-treatment or post-nonsurgical endodontic therapy (30, 31). Data from these studies suggests that periapical lesions underwent reduction in volume beyond the first year post-treatment and that further healing was likely to occur with persistent defects (31). A retrospective radiographic and clinical outcomes study of ninety-five cases suggests that pre-operative volumetric assessment may have predictive value in endodontic microsurgery; lesion volumes greater than 50 cubic millimeters were found to be a significant negative predictor at a 1-year recall (32).

Volumetric changes in periapical lesions visualized on CBCT post-apicoectomy have not yet been sufficiently addressed, and it appears that long-term follow-up over the course of several years may be necessary to observe the extent of post-operative healing with some studies reporting that the process may take up to 4 years (33). Establishing a post-surgical timeline for the resolution of periapical lesions not only has diagnostic utility but also may inform a dental care provider's clinical decision regarding the next phase of treatment for the involved tooth.

The aim of this study was to evaluate whether volumetric changes in persistent periapical lesions can be detected in long-term follow-ups after apicoectomy using cone-beam computed tomography. The null hypothesis, H_0, is that no volumetric differences will be observable

4

between pre- and post-operative CBCT imaging of periapical lesions. The alternative hypothesis,

H_a, is that an observable volumetric pre- and post-operative difference exists.

Materials & Methods

This study was a review of secondary data using a prospective cohort design to determine the post-surgical dimensional changes that occur in periapical radiolucencies using CBCT. The VCU Institutional Review Board approved the study (IRB #HM20006374). Patients with a previous treatment history of apicoectomy performed at VCU and for whom a pre-operative CBCT scan was taken between November 2010 and December 2015 were eligible for inclusion and recalled to the graduate endodontic practice at the VCU School of Dentistry.

The study population comprised patients who presented for endodontic treatment in the Graduate Endodontic Practice at VCU School of Dentistry (Richmond, VA). Patients were referred for evaluation and treatment from the VCU School of Dentistry undergraduate student clinics as well as the Advanced Education in General Dentistry residency, Faculty Practice, and Richmond metropolitan private dental practices.

Graduate endodontic residents completed the initial pre-surgical evaluations of all patients. Evaluations included patient-reported subjective information, clinical exam findings, diagnostic test results, and radiographic analysis. Pulpal and periapical diagnoses were rendered post-evaluation. This information was recorded in each patient's electronic health record (axiUm®) and included the following data:

Subjective Symptoms: pain to cold or heat thermal stimulus, pain on biting or release, localizable or diffuse pain

<u>Diagnostic Testing</u>: cold thermal test, bite test, percussion test, transillumination, mobility, probing depths

<u>Radiographic Evaluation</u>: presence or absence of a periapical radiolucency, estimated size of the periapical radiolucency, periodontal defects present (isolated, generalized, vertical, horizontal), proximity of lesion to sensitive anatomic structures (e.g. maxillary sinus, mental foramen, inferior alveolar nerve canal)

<u>Diagnosis</u>:

Pulpal: symptomatic irreversible pulpitis, asymptomatic irreversible pulpitis, pulpal necrosis, previously treated, previously initiated therapy

Periapical: normal periapical tissues, symptomatic apical periodontitis, asymptomatic apical periodontitis, acute apical abscess, chronic apical abscess, condensing osteitis

Surgical treatment was performed in accordance to standard clinical protocol. Reflection of a full-thickness mucoperiosteal flap preceded osteotomy and root resection in all included surgical cases. In most, but not all surgical cases, roots were ultrasonically retroprepared prior to placement of a retrofill material. Intra-operative hemostasis was achieved with the use of standard cotton pellets, epinephrine-impregnated cotton pellets (Racellets®), and/or ferric sulfate. Flap closure was achieved via monofilament suture materials. All cases were completed with the use of a Zeiss OPMI® Pico microscope.

Patients were included in the study if (1) documentation of their clinical records was complete, (2) surgical treatment was completed on at least one of their teeth, (3) and a pre-surgical CBCT was taken, showing evidence of an area of low density around the apex of at least one root of the affected tooth/teeth in question. An area of low density (or radiolucency)

periapically was defined as a lesion if it measured at least twice the width of the normal periodontal ligament space on an adjacent healthy tooth.

Patients who were pregnant, had a history of receiving therapeutic radiation to the head or neck, were younger than 18, or older than 89, were excluded from the study. Those patients for whom graft material was placed in the surgical access site were excluded due to obfuscation of periapical lesion volume on CBCT. There was no eligibility restriction based on factors related to race, ethnicity, or sex.

In compliance with standard clinical practice, all included patients were enrolled in the post endodontic treatment recall system in the graduate practice. Patients, who met the inclusion criteria, were asked to return to the graduate practice for a recall appointment. The recall visit included a clinical and radiographic evaluation for the tooth/teeth in question. Data collected at the recall visit included: patient demographics (age/sex), physical status classification via American Society of Anesthesiologists (ASA) scoring, initial date of surgery, and operative sextant/tooth/teeth. Patients were provided information about the study and given the option to voluntarily participate. If patients opted to enroll in the study, they were provided a copy of the study consent form to read and sign. Study participants were compensated $35.00 in cash. For participants, a follow-up CBCT and periapical radiograph were obtained. No clinical protocol was altered for the sake of the study.

After obtaining informed consent for study participation, a limited field of view (5x5 cm) CBCT scan at a voxel size of 0.090 mm was taken of the post-operative site for each recalled patient, using the Carestream 9300 system (Carestream Health; Rochester, NY). Operating parameters were set at 2-10mA, 60-90 kV, and 12 seconds. CBCT scans were analyzed using a

Dell Optiplex 990 computer (Dell SA, Geneva, Switzerland) and a 22-inch LCD monitor with a

resolution of 1680 x 1050 pixels (Dell SA, Geneva, Switzerland).

Volumetric analysis of Pre- and Post-op CBCT scans were completed by two calibrated

and blinded evaluators—a board-certified oral and maxillofacial radiologist and a board-certified

endodontist—under identical viewing conditions using CS 3D Imaging software (Carestream

Health; Rochester, NY). Each evaluator was given a copy of the Protocol for Linear

Measurement of Lesions (see Appendix A). Post-operative healing was assessed via linear

measurement of maximal periapical lesion dimensions in all three orthogonal planes whereby

each evaluator was asked to make a measurement from a bone landmark to another bone

landmark across the void of the lesion. If the lesion of interest did not demonstrate clearly

demarcated boney borders (e.g. cortical plate perforation of the lesion, direct sinus involvement),

each evaluator was asked to estimate the lesion boundary by interpolating the lost bony contour.

A calibration between evaluators was performed by comparing the measurements made on the

first four lesions in the study.

The linear measurements of the lesions were as follows: In the coronal plane, the

maximum coronal diameter (MCD) was determined from the largest extent of the lesion. And

then the largest height perpendicular to this direction was recorded as the minimum coronal

diameter. Then in the sagittal plane the maximum sagittal diameter (MSD) and minimum sagittal

diameter was determined. And finally, in the axial plane, the maximum axial diameter (MAD)

and minimum axial diameter was determined. In each view, the coronal, sagittal and axial, the

area of a lesion was calculated as follows: The area of an ellipse with the principle axes (radii) of

length a, and b—half the measured diameters—was calculated as Area = $\dfrac{\pi}{4}ab$. The volume of

the lesion was calculated as follows: The volume of an ellipsoid with the principle axes (radii) of

length *a*, *b*, and *c* is calculated as Volume $= \frac{4}{3}\pi abc$, using the largest of the pair of diameters as

twice the radii in this formula.

To describe the extent of the change in diameter, area, or volume the ratio of the Post-op

value to the Pre-op value was used. The percent change was calculated 100 times the difference

between the Pre-op value and the Post-op value divided by the Pre-op value.

After the evaluator made the measurements of the pre- and the post-surgical scans, the

evaluators made an evaluation of the change in post-surgical lesion size using criteria for the

combined apical-cortical area (B-score) as suggested by Von Arx et al. (25). Inter-rater reliability

was assessed via Kappa statistics.

An endodontic resident measured each pre- and post-surgical periapical radiolucency

using DiThreshGUI (DTG) software (DiThreshGUI 1.4)—a CBCT volumetric software

developed by Anthony Fouad. The software relies on a two plane cross-correlation method to

determine the volume in addition to the maximum coronal, sagittal, and axial diameters of

periapical lesions (DiThreshGUI Lesion Protocol is in Appendix B). Data from each

measurement was compiled using Microsoft Excel (Microsoft Corp. Redmond, WA).

In order to compare manual volumetric measurement against software output, two

analyses were performed using a repeated-measures ANOVA. The first tested whether the mean

volumes were different as measured on Pre- and Post-op CBCT scans. The second tested the

correlation between the two volumetric assessment methods. Additionally, an analysis was

performed to test whether the amount of volumetric change across time was the same for the two

methods.

Volume measurements from the linear measurements are in mm^3 units and the DTG

volume measurement from the software is in voxels. Since individual volume measurements may

be subject to skewed data points, the cube root was used for analysis and then the results were

back-transformed to the original scale for presentation.

Results

The results of this study begin with a description of the patients and the teeth studied. The next section addresses the primary aim of the study as it focuses on the change in the lesion volume across the two time points termed Pre-op and Post-op (recall). This section also includes a description of the relationship between volumes determined by the software and volumes calculated by the linear measurements obtained from the two evaluators. Each evaluator was asked to characterize the healing status of the lesion, and this is described in the third section. In following sections, the linear measurements obtained from each rater and the associated calculated areas and volume are presented. Finally, a section on the data obtained by the DTG measurement of diameter and volume is presented.

Description of Patients and Teeth

Eighty-six patients were identified as having met the inclusion criteria; 6 patients declined citing personal reasons and 4 patients had moved out of the state. Three patients scheduled post-surgical recall visits but failed to show up for their appointments. Seven patients reported having the tooth of interest extracted for unspecified reasons. Forty-six patients could not be reached by phone despite numerous attempts to contact them for recall visits. Twenty patients returned for recall appointments and consented to participation in the study. As such, the recall rate was 23.2%.

The demographic information obtained from the participants are shown in Appendix C. The participants (n=20) had an average age of 65.9 years (SD = 9.6, range = 46 to 84). The 9 females and 11 males were followed up after an average of 37 months (SD = 16.7, range = 13 to 63 months). These patients had a total of 27 treated teeth. Thirty percent (n=6) were ASA=1, 60% (n=12) were ASA=2, and the remaining 10% (n=2) were ASA=3. Complete data compiled for the 20 participants and 27 separate teeth can be found in Appendices D and E.

Table 1. Teeth in the Study

Tooth Type		Mandibular	Maxillary	Total
Incisor	L1	1	4	5
	L2	0	5	5
Canine	C	1	3	4
Premolar	P1	0	3	3
	P2	0	3	3
Molar	M1	5	2	7
	M2	0	0	0

Lesion Volume

The volumetric data obtained from the software are show in Appendix D. Volume, maximum coronal diameter (MCD), maximum sagittal diameter (MSD), and maximum apical diameter (MAD) were determined. Using volume calculated from the software, 24 lesions showed a reduction in volume at recall, and 3 lesions showed volumetric increase. The Pre-op volumes ranged from 800 to 697,251 voxels with a median value of 79,348 voxels, which is less than the mean value of 163,496. The Post-op volumes ranged from 0 to 268,372 voxels with a median value of 10,830 voxels, which is less than the mean value of 36,154 voxels. Figure 1 shows the distribution of the volume measurements on the two occasions and Figure 2 shows that the majority of the lesions decreased in volume.

13

In Figure 1, each dot represents a periapical radiolucency. Dots below the diagonal line showed a decrease in size and dots above the line showed an increase in size. In Figure 2, the change in volume is shown for each lesion. Specific time intervals are not identified.
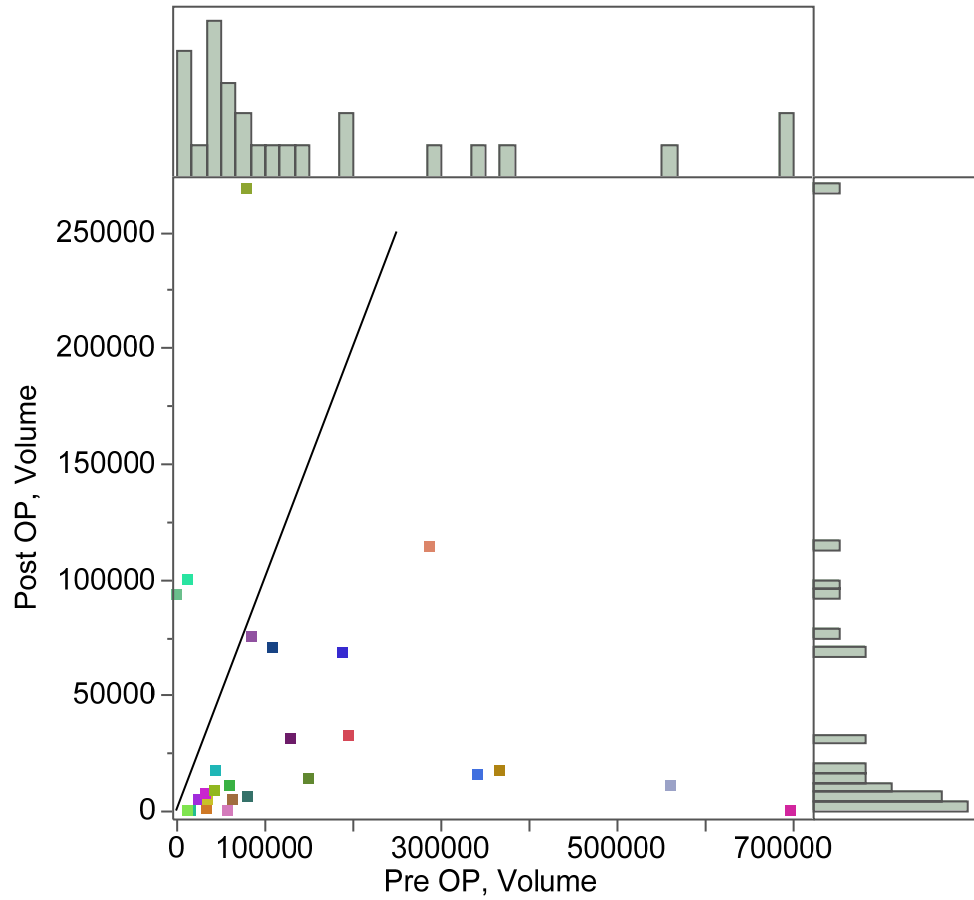
Figure 1. Distribution of Volume Measurements
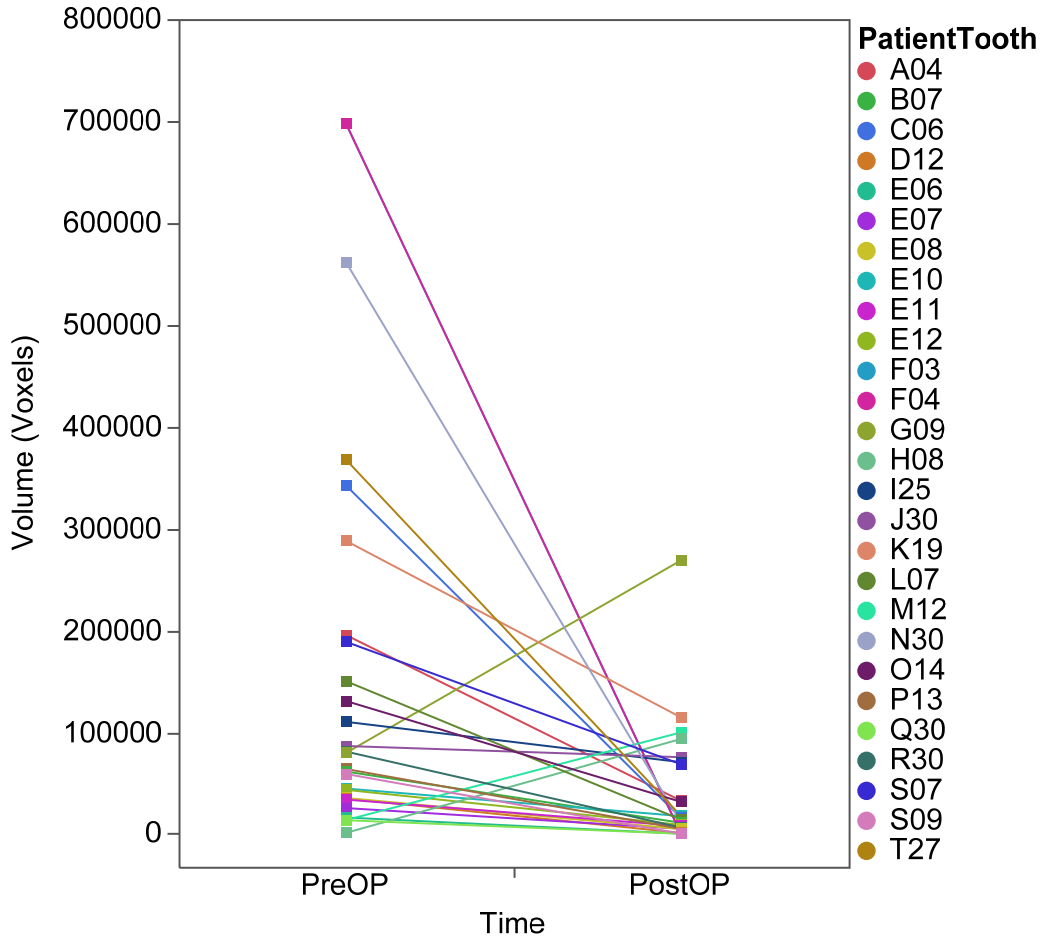
Figure 2. Change in Pre-op and Post-op Volumes Measurements

The linear measurements of the two evaluators can be found in Appendix E. The linear measurements were used to calculate the volume of the 27 lesions using the maximum diameters and an ellipsoid mathematical model. Similar to the volumes obtained using DTG, the volumes, obtained from the linear measurements, were strongly skewed by large outlier lesions. The Pre-op volumes ranged from 0 to 6113mm^3 with a median value of 534 mm^3, which is less than the mean value of 1080 mm^3. The Post-op volumes ranged from 0 to 993mm^3 with a median value of 3.8 mm^3, which is less than the mean value of 130 mm^3. Figure 3 illustrates the distribution of the volume measurements on the two occasions. Lesions below the diagonal line decreased in size, and those few above the diagonal increased in size. The change in volume can be better

15

seen in Figure 4. What is apparent is that most lesions decrease in size, but some remain the

same size and fewer still increase. The Post-op follow-up time intervals vary by patient.
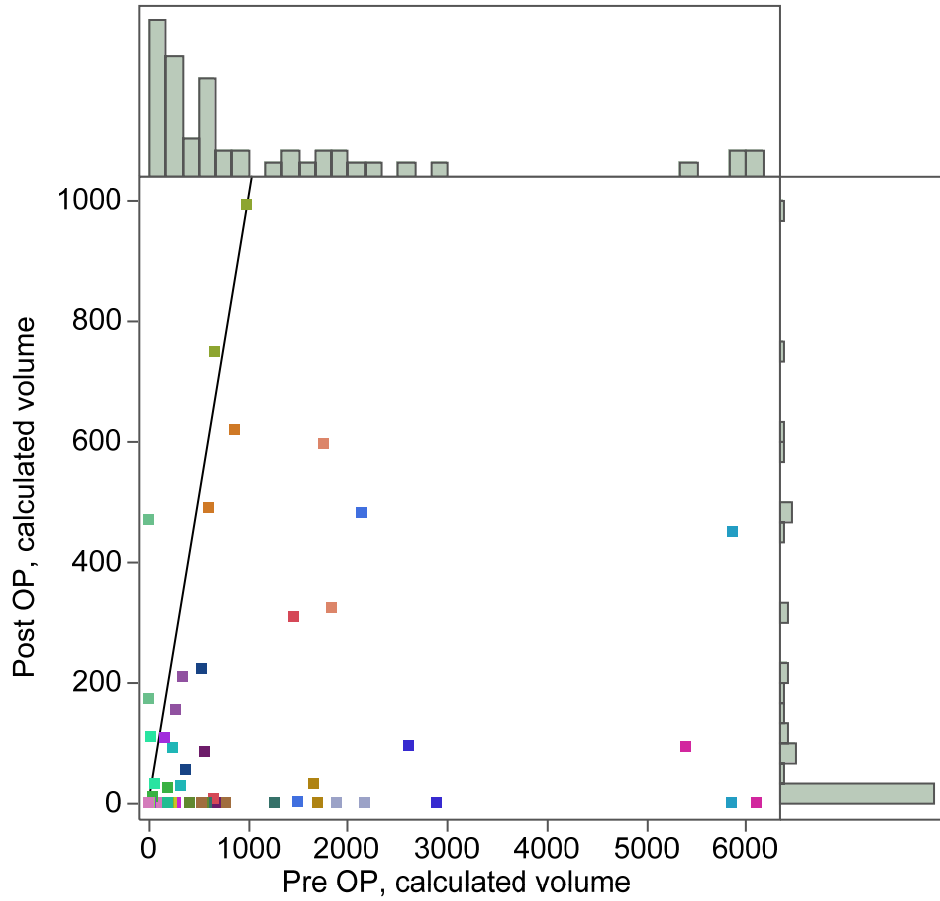
Figure 3. Pre-op and Post-op Volumes Calculated by the Linear Measurements
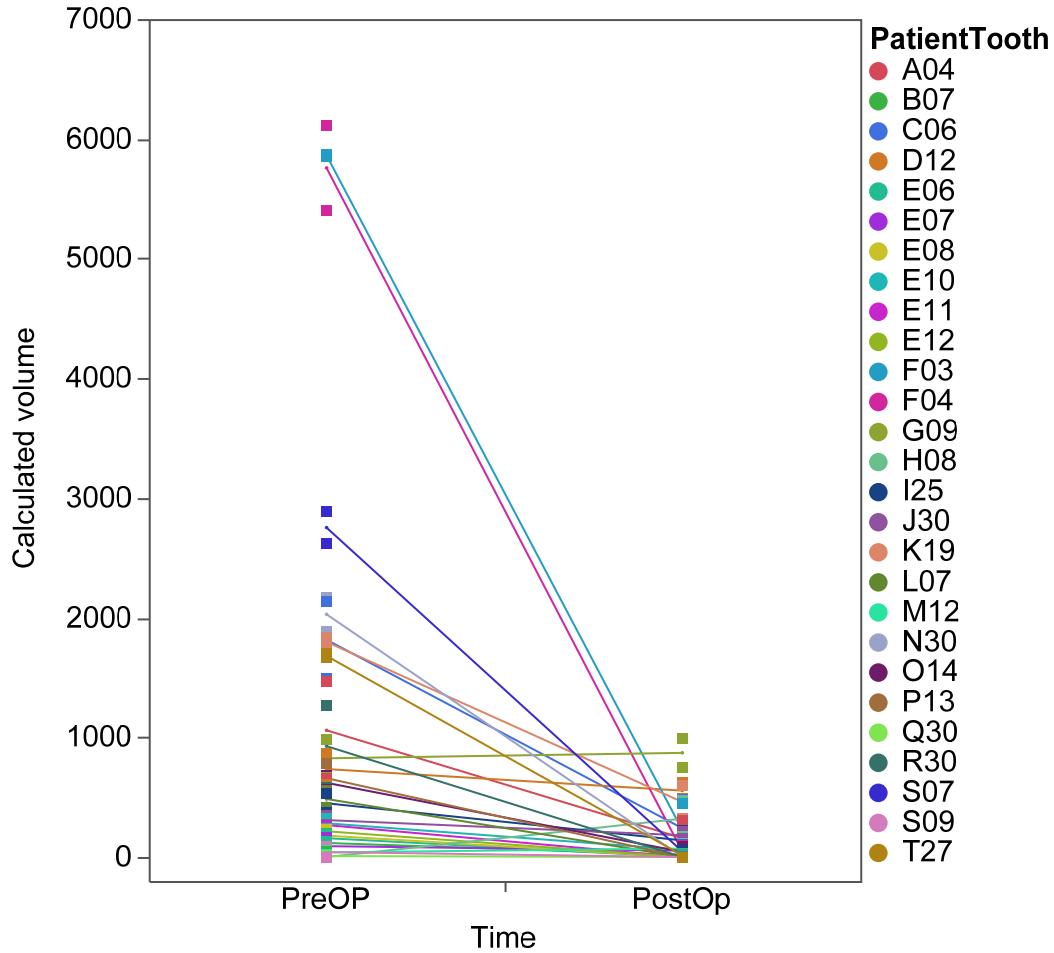
Figure 4. Change in Pre-op and Post-op Volumes Calculated by the Linear Measurements

To deal with the skewed values, the cube-root of the volume measurements were analyzed using repeated-measures mixed model ANOVA. Overall, the volumes significantly decreased using both the DTG measurement of volume ($P = .0002$, Table 2) and volume calculated from the linear measurements ($P < .0001$). For the DTG volume measurements, the average volume decreased from 102,130 voxels to 14,337 voxels, a change of 86%. For the linear-derived volume measurements, the average volume decreased from 559mm^3 to 23mm^3—a change of 96%.

Table 2. Pre-op and Post-op Volumes

Occasion	Volume	95%CI		P-value
DTG Volume Calculation				
Pre-op	102,130	(58,355	to 163,655)	
Post-op	14,337	(5,524	to 29,531)	
Ratio	0.14			0.0002
Change	0.86			
Volume Calculated from Diameters				
Pre-op	559	(275	to 991)	
Post-op	23	(5	to 61)	
Ratio	0.04			<.0001
Change	0.96			

A repeated-measures mixed-model ANOVA was performed on the cube-root transformation. Estimates were obtained by back-transforming the estimates.

Three volumetric measurements were obtained—one obtained via the software and two linear-derived volumes obtained by the radiologist's and endodontist's measurements. In addition to the difference between the units (mm^3 vs. voxels), the measurement of volume is not identical by the three measurements. Figure 5 shows the correlations between the three measurements at Pre-op and Post-op. Note that the cube-root scale is used for each data set to make these measurements approximately normal and, thus, the correlations meaningful. All of the Pre-op measurements are strongly correlated ($r > 0.88$) and all of the Post-op measurements are moderately correlated ($r > 0.47$). It is to be expected that the correlations across the two occasions are reduced. There also is substantial agreement between the Pre-op vs Post-op ratios as shown in Figure 6. Note, however that since there were three instances where the Pre-op volume was zero, the ratio is undefined.

	PreOP, DTG	PreOP, #1	PreOP, #2	PostOP, DTG	PostOP, #1	PostOP, #2
Pre-op, DTG	1.00	0.92	0.88	-0.10	0.08	-0.05
Pre-op #1	0.92	1.00	0.95	-0.10	0.25	-0.03
Pre-op, #2	0.88	0.95	1.00	0.00	0.23	0.04
Post-op, DTG	-0.10	-0.10	0.00	1.00	0.47	0.62
Post-op, #1	0.08	0.25	0.23	0.47	1.00	0.57
Post-op, #2	-0.05	-0.03	0.04	0.62	0.57	1.00
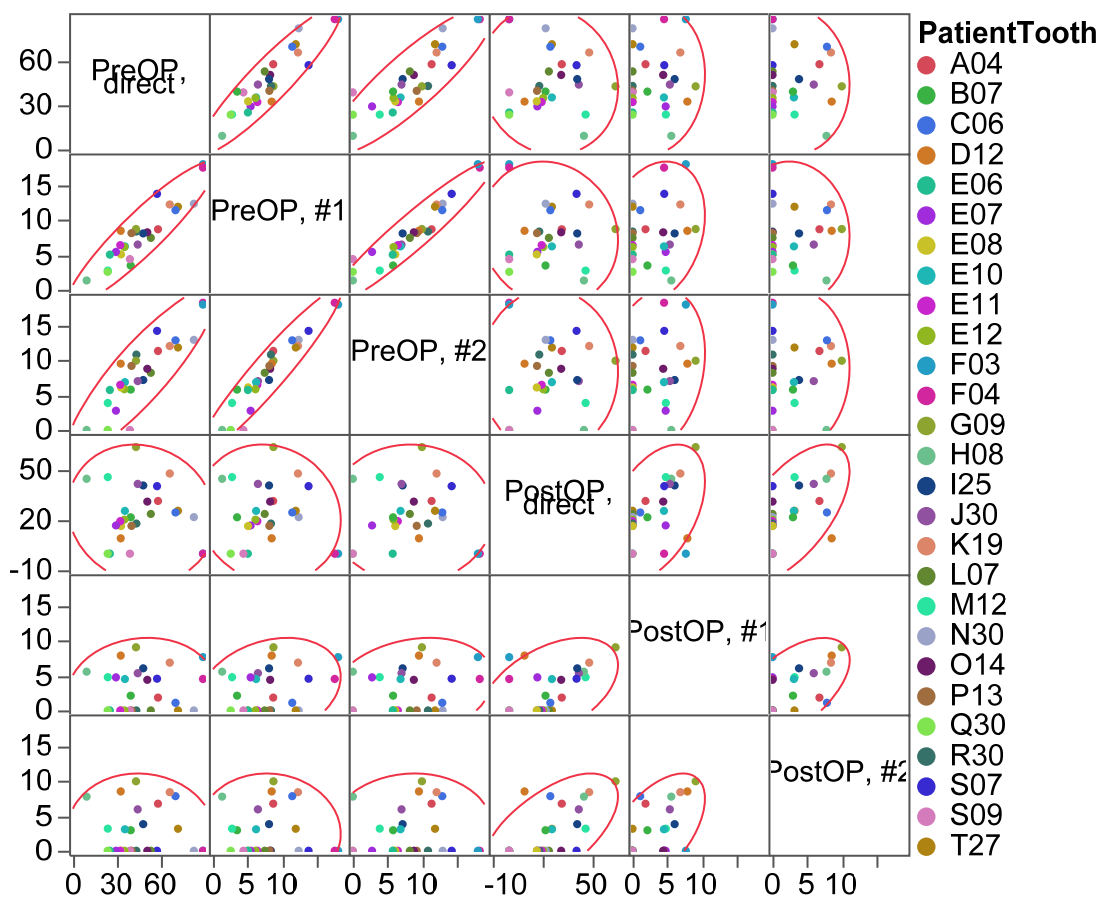
Figure 5. Correlation between the Volume Measurements (cube-root scaling)

	Ratio One	Ratio Two	Ratio Volume
Ratio One	1.00	0.99	1.00
Ratio Two	0.99	1.00	0.99
Ratio Volume	1.00	0.99	1.00
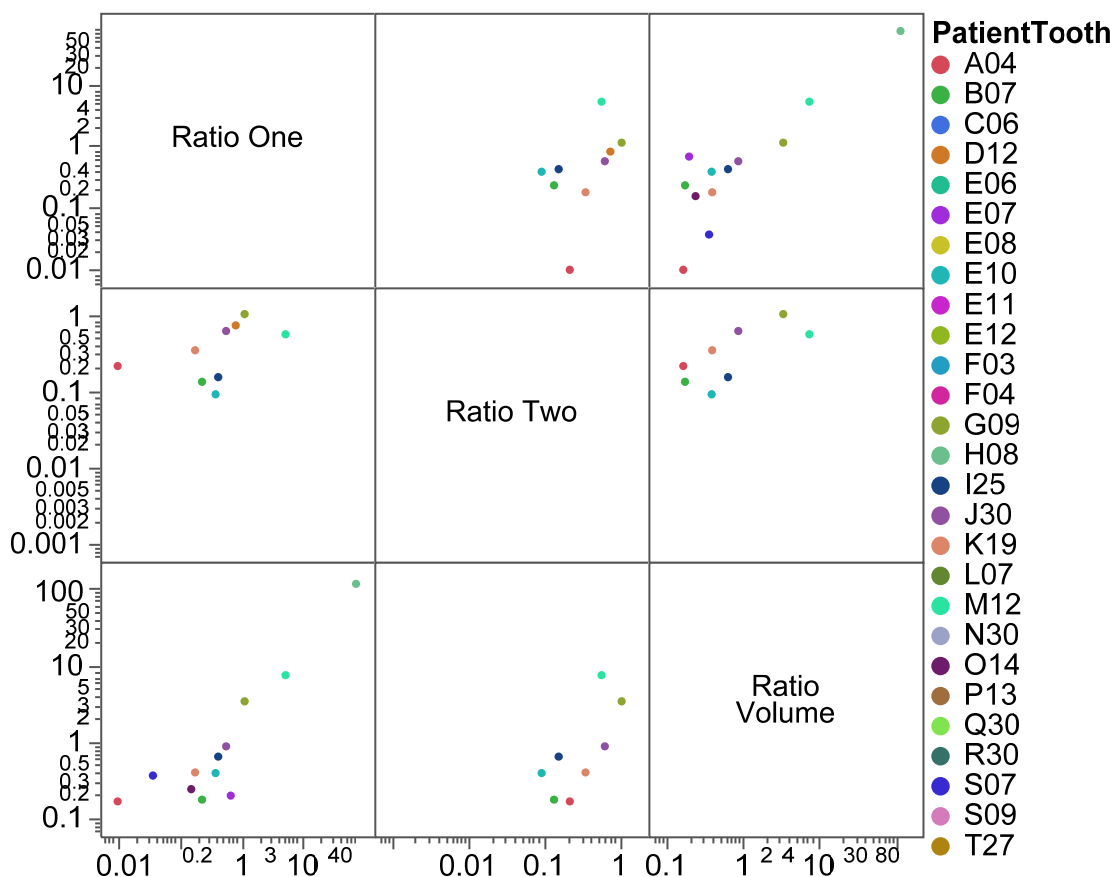
Figure 6. Correlation between the Pre-op vs Post-op Ratios

Healing Status

After making the linear measurements, the two raters were asked to characterize the pair

of readings in a B-score to represent "No healing", "In between", or "Healed." They agreed in

56% of the cases, with a significant chance-corrected agreement (Kappa = 27%, P = 0.032 Table

3).

Table 3. Agreement on Change in Volume

| | Rater #2 | | | |
Rater #1	No healing	In between	Healed	Total
No healing	2	2	0	4
In between	1	6	6	13
Healed	0	3	7	10
Total	3	11	13	27

56% agreement; Kappa = 27% (P = 0.032)

Linear measurements and calculated areas and volume

Two examiners, a radiologist and an endodontist recorded the linear measurements. They each independently determined the largest width of the lesion on the axial view (Axial 1) and then determined the largest height perpendicular to this width (Axial 2). Then, in similar manner the Sagittal 1 and Sagittal 2 measurements were made and the Coronal 1 and Coronal 2 measurements made. On the nine occasions when the radiologist did not give a measurement, a zero value was used. The summary descriptive statistics for the measurements are shown in Table 4 and visually presented in Figure 7.

Figure 7 and the correlations indicate that all of the linear measurements are strongly related—that measuring "lesion size" in any view will yield similar results. A multivariate ANOVA of the six measurements indicated that there was no significant difference between the two raters (P = 0.2084).

21

Table 4. Descriptive Statistics of the Linear Measurements

Measurement	Mean	Std Dev	Range	
		Pre-op		
Sagittal, max	5.49	3.08	0	12.0
Sagittal, min	4.11	2.69	0	10.2
Coronal, max	5.37	3.08	0	12.3
Coronal, min	3.94	2.44	0	11.3
Axial, max	4.82	2.77	0	10.6
Axial, min	3.64	2.29	0	9.5
		Post-op		
Sagittal, max	2.03	2.34	0	8.7
Sagittal, min	1.34	1.72	0	5.8
Coronal, max	2.12	2.33	0	8.0
Coronal, min	1.20	1.51	0	5.8
Axial, max	1.43	1.97	0	5.1
Axial, min	0.94	1.42	0	4.3

Correlations

	Sagittal, max	Sagittal, min	Coronal, max	Coronal, min	Axial, max	Axial, min
Sagittal, max	1.00	0.93	0.90	0.85	0.85	0.85
Sagittal, min	0.93	1.00	0.88	0.90	0.85	0.89
Coronal, max	0.90	0.88	1.00	0.90	0.86	0.86
Coronal, min	0.85	0.90	0.90	1.00	0.86	0.92
Axial, max	0.85	0.85	0.86	0.86	1.00	0.95
Axial, min	0.85	0.89	0.86	0.92	0.95	1.00
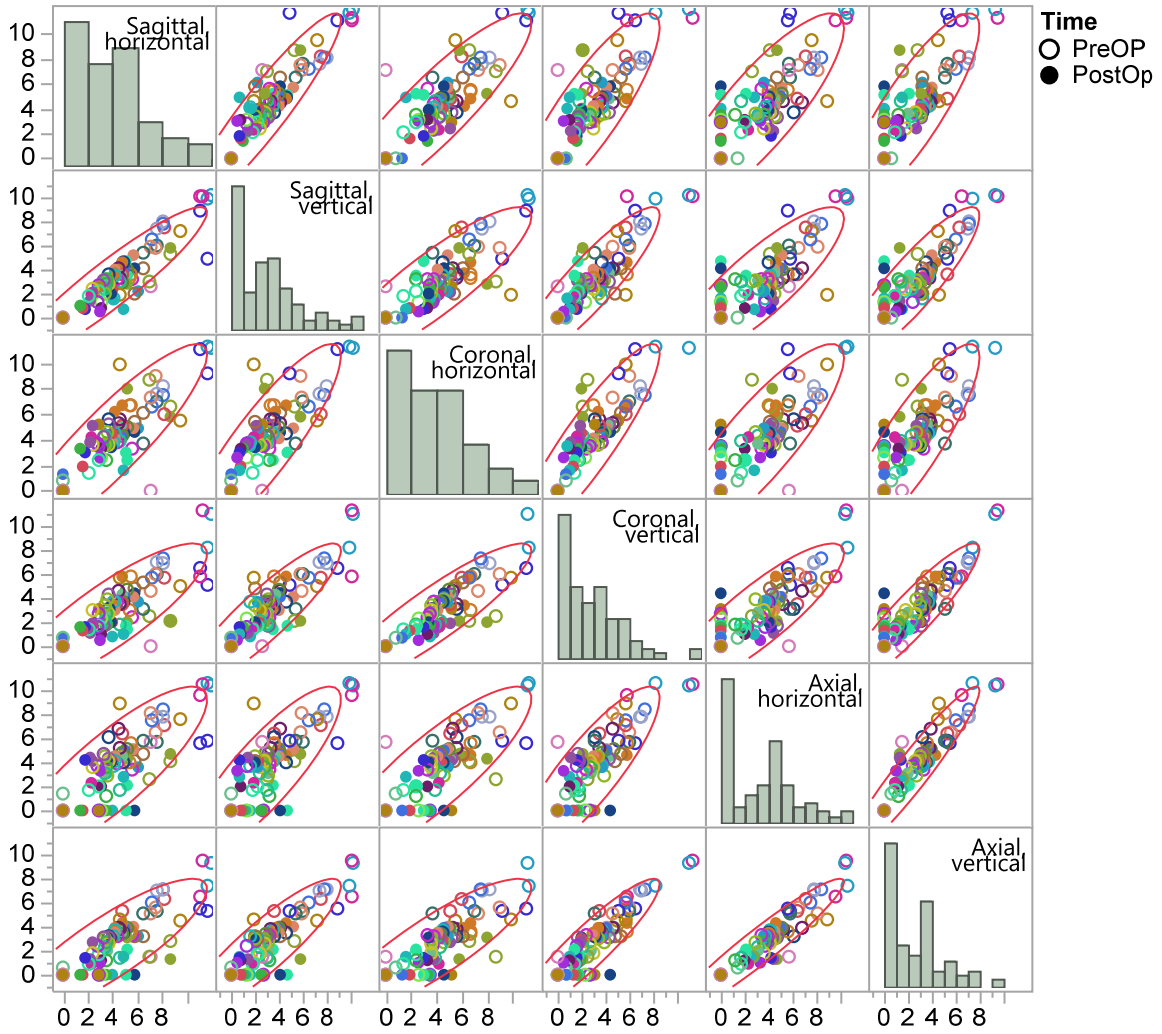
Figure 7. Relationships between the Linear Measurements

In each view, the coronal, sagittal and axial, the area of a lesion was calculated using the linear

measurements. The summary statistics for the three areas are shown in Table 5 and the

relationships between the three are depicted in Figure 8. Note that all the areas are rather skewed;

therefore, the summary statistics are affected by the outliers.

Table 5. Descriptive Statistics for Area

Area	Mean	Std Dev		Range
		Pre-op		
Sagittal Area	23.51	25.59	0	96.1
Coronal Area	21.59	23.00	0	109.2
Axial Area	18.31	18.55	0	78.3
		Pre-op		
Sagittal Area	4.97	7.93	0	39.6
Coronal Area	4.37	6.52	0	30.5
Axial Area	3.06	4.98	0	16.0

Correlations

	Sagittal Area	Coronal Area	Axial Area
Sagittal Area	1.00	0.90	0.89
Coronal Area	0.90	1.00	0.94
Axial Area	0.89	0.94	1.00
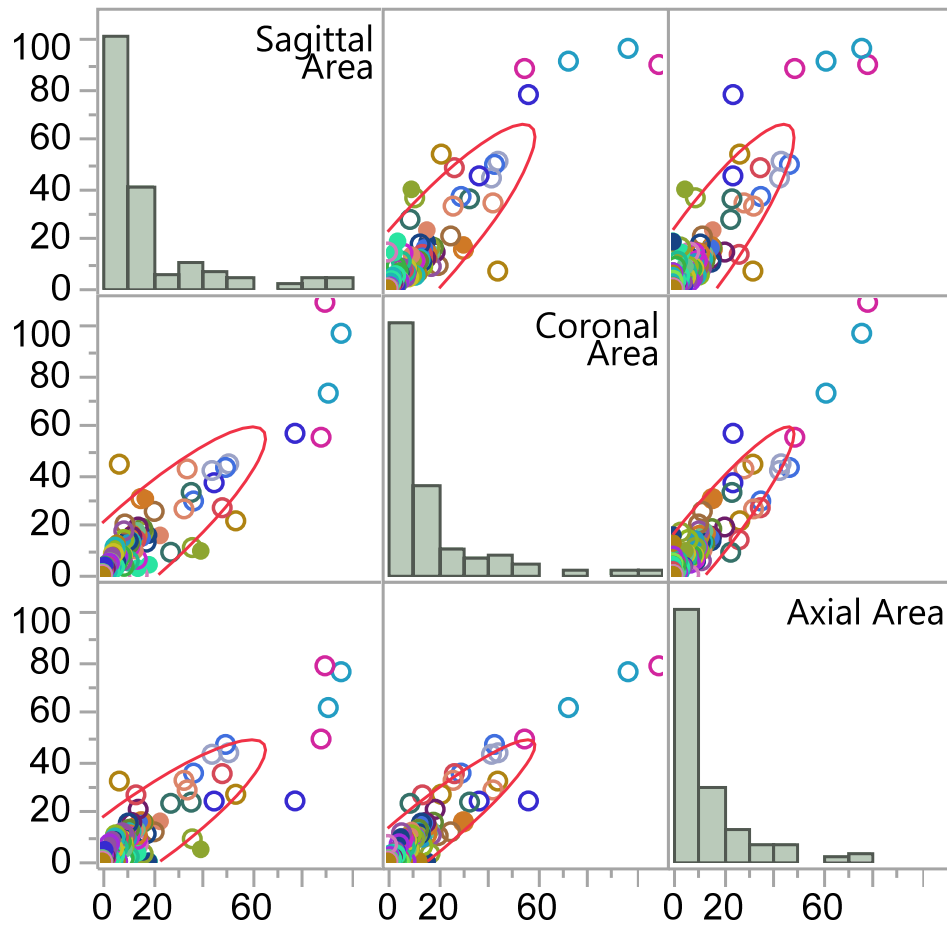
Figure 8. Relationships between Area Calculations

The volume of an ellipsoid (with the principle axes corresponding to half the linear diameters) was calculated from the linear measurements. Figure 9 shows the relationships between each of the areas and calculated volume.

Volume By Axial Area

Volume By Sagittal Area

Volume By Coronal Area
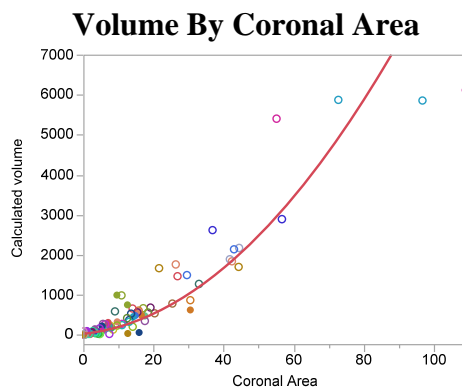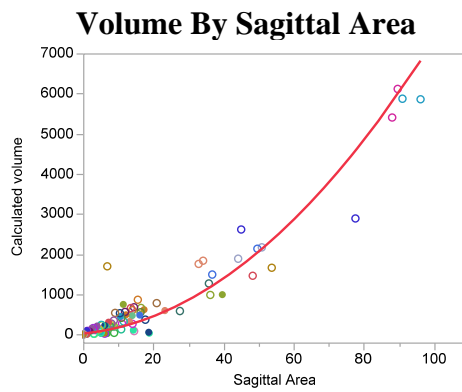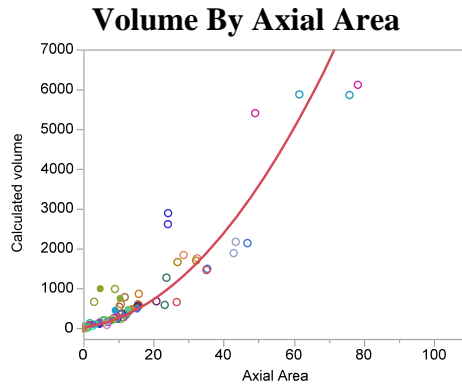
Figure 9. Relationships between Three Areas & Volume

The measurements of volume by the DTG method resulted in a database with measurements for each person and occasion. Four variables were recorded: Max coronal diameter, Max sagittal diameter, Max axial diameter, and Volume (voxels). Table 6 shows the average, SD and range of values of each variable. The diameters are normally distributed but volume clearly is strong skewed (see Figure 10). One result of the skewed volume measurements is that the mean is strongly affected by the outliers; the mean (99,825) is much larger than the median (34,840).

Table 6. Descriptive Statistics for the Volume Measurements

Variable	N	Mean	Std Dev	Minimum	Maximum
Sagittal	54	57.33	32.71	0	136
Coronal	54	45.70	28.84	0	134
Axial	54	44.31	32.54	0	137
Volume	54	99825.10	160837.00	0	697251

Correlations				
	Sagittal	Coronal	Axial	Volume
Sagittal	1	0.8228	0.7542	0.7172
Coronal	0.8228	1	0.8949	0.876
Axial	0.7542	0.8949	1	0.8469
Volume	0.7172	0.876	0.8469	1
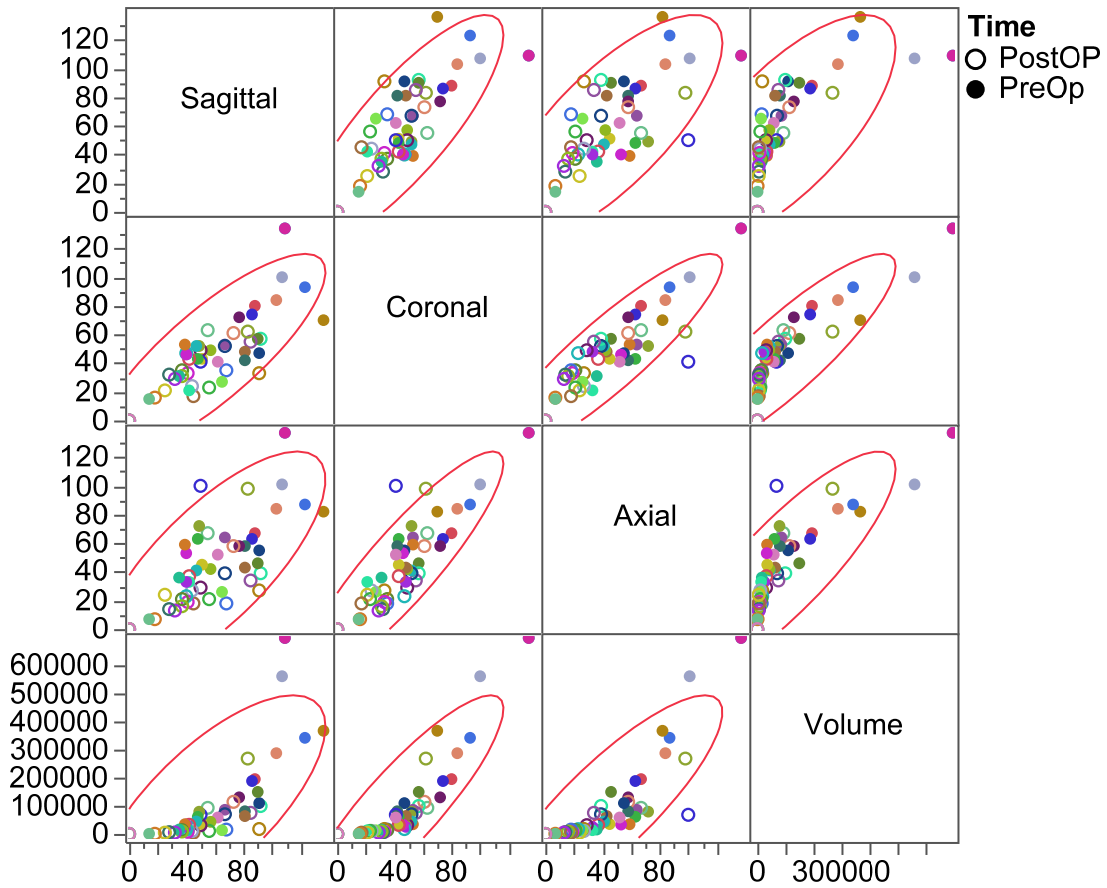
Figure 10. Relationships between the DTG Measurements

There is a relationship between each of the diameters and volume (see Figure 11), but the relationship is not linear. The curve in the figure is the result of fitting a straight line on the log scale of each variable. These figures illustrate that the DTG algorithm relies on the surveyed diameters on each view.

VOL (voxels) By Max coronal diameter
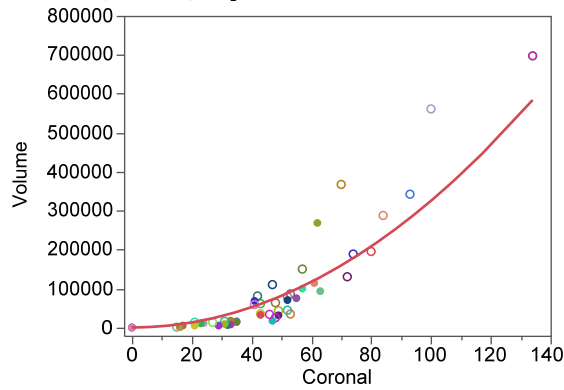
VOL (voxels) By Max sagittal diameter
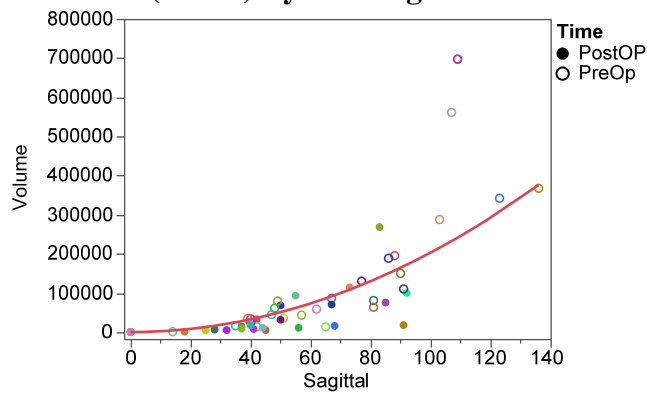
VOL (voxels) By Max axial diameter
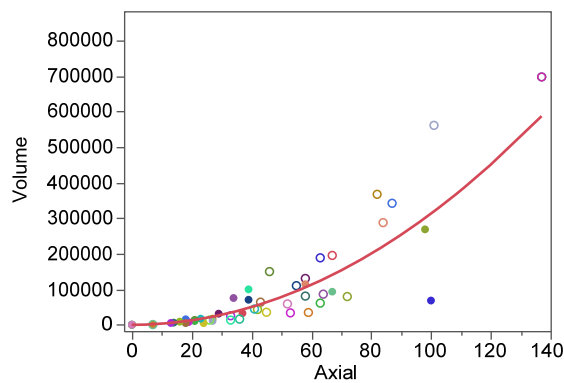
Figure 11. Relationships between the DTG Diameters and Volume

As an additional check, the volume of the lesion may be calculated from the three diameters and this compared to the DTG volume calculation. Figure 12 shows that there is a strong correlation (Spearman's rho = 0.84) but the scale is different. Note that the scatterplot is shown on the log scale. Given that zero volume data points result in an undefined value on a log

scale, figure 12 score these volumes as 1. The median DTG volume is 34,841 voxels whereas the

linear-derived volume is much smaller (median = 110mm^3).
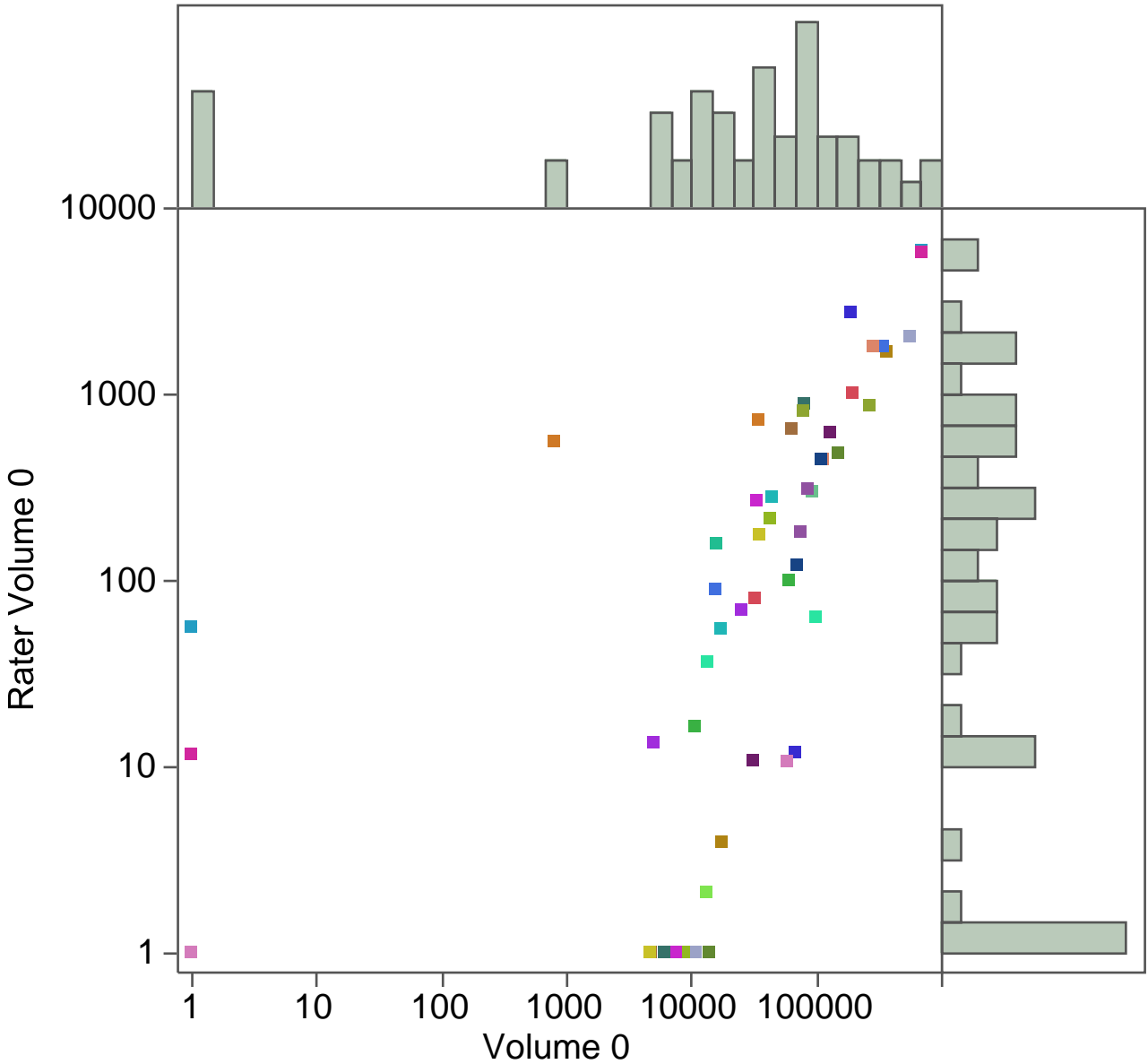
Figure 12. Calculated Ellipsoidal Volume by DTG Volume (voxels)

Replicability

Four teeth were measured twice and may be used to indicate the replicability of the

measurements. The six linear measurements on these participants were analyzed using a multi-

way ANOVA with patients and measurements as effects in the model. The mean squared error

from this model indicted that the variation across the replicates was 0.985mm, where the average

measurement was 4.6mm. Given a larger scale of measurement, the three diameters measured

using the DTG software had an average of 65.7 units. The mean squared error in this situation

was 8.8 units.

Discussion

The statistically significant reduction in size of periapical lesions, if taken to be a proxy of surgical success, was observed in this study for 24 out of 27 teeth (88%). This success rate appears to be in line with what has been reported for surgical outcomes with modern techniques (9). It is noteworthy that 2 of the treated teeth underwent apicoectomy without follow-up retropreparation or retrofill and nonetheless demonstrated evidence of apical healing.

Post-surgical healing is a dynamic process affected by factors of patient health. The majority of patients (90%) recruited to participate in this study were classified as either ASA 1 or 2. The average age of patients in this study—65.9 years—may reflect delayed treatment planning of apical surgery as a sequential third-line option after failure of non-surgical treatment and follow-up retreatment. The generalizability of this study's results may be limited in younger cohorts or patients with pervasive systemic health issues.

The average recall time interval in this study was 37 months, which may be appropriate given recent findings of peak incidence of healing. Notably, CBCT studies have found relatively low rates of complete healing one year after endodontic treatment (33). While one study by Patel et al. reports resolution of approximately 48% of lesions at one year post-operatively, contradictory results have been published independently by Liang and van der Borden in the range of 19% and 16%, respectively (34-36). Relatedly, another study suggests that approximately 22% of periapical lesions that failed to demonstrate evidence of complete healing after one year post-treatment did so at the two-year follow-up (37).

32

To date, several studies have attempted to either describe or quantify changes in the size of periapical lesions using CBCT. Orstavik is credited with the development of a periapical index for interpretation of periapical lesions on radiographs (38). This index, in turn, paved the way for Estrela et al. to adapt a similar 6-point system for CBCT scans (39). A 2013 study was among the first clinical investigations that sought to use a CBCT-assisted volumetric analysis of periapical lesions in the assessment of outcomes for traditional nonsurgical root canal treatment (35). In keeping with the measurement of post-surgical healing outcomes as proposed by Von Arx et al. (25), the results of this study indicate that use of the B-score is feasible in clinical settings but its scale requires closer examination.

While 56% agreement between evaluators appears to reflect a lack of diagnostic calibration, it is worthwhile to note that none of the 27 sampled teeth were simultaneously scored at opposite ends by the two evaluators; in other words, all of the evaluated lesions were accorded B-scores within 1 point of each other on the 3-point scale of healing. This single point discrepancy may be attributed to the wide qualitative middle range that defines a B-score of 1 in which post-surgical hard tissue fill occurs either with or without cortical plate reformation—all to some limited degree less than complete healing.

The pre-operative linear measurements were found to be strongly correlated between evaluators while the post-operative values were only moderately so. This discrepancy may, in large part, be due to the tendency for pre-operative lesions to be large in size and also present with significant variance. This large deviation from a mean value in lesion size allow calibrated evaluators to execute similar dimensional measurements with a large margin for error. Post-operative (or healing) lesions however tend to be small with little variance, which magnifies differences in linear measurements obtained by each evaluator.

Though calibrated to the measurement protocol, the evaluators in this study are also subject to the experiential biases of their respective training in endodontics or oral radiology as they pertain to assessment of lesion healing. In one particular case, the endodontist evaluator diagnosed the post-surgical formation of an apical scar with a small but persisting through-and-through lesion at its center, therefore awarding a B-score of 1. The oral radiologist noted that this area of low density was dimensionally similar to that of the Pre-op lesion, resulting in a B-score of 0. Several studies in the endodontic literature have pointed to the role of biases in the interpretation of radiographs (40, 41). The results of this study suggest that evaluator bias may also be a significant contributor to outcomes assessment via CBCT.

Software-based volumetric analysis of periapical lesions on CBCT scans have only recently gained traction in the endodontic literature with each platform relying on a different algorithm (28, 29). DTG volumetric software was developed by Anthony Fouad using MATLAB—a numerical computing environment and programming language. DTG relies on a geometric boundary established by an evaluator and a grayscale-based biplanar cross-correlation method to output lesion volume. To test the clinical validity of DTG, a University of Maryland pilot study relied on the creation of artificial bone lesions in a dry skull at the apices of intact teeth (42). Carestream Kodak 9000 and Planmeca Promax CBCT machines were used to image the dry skulls prior to deployment of the DTG software for volumetric assessment of each lesion. For an objective standard, polyvinylsiloxane impressions were taken of each artificial lesion and a water displacement method was used to determine the volume of the impression and lesion by proxy. The pilot study concluded no significant difference in the volume measurement between the tested groups and that the DTG-assisted volumetric analysis yielded an accurate representation of the true periapical lesion volume.

In our study, DTG volumetric analysis of periapical lesions were found to be sensitive to the changes that typically occur post-surgically. This analysis was also found to be correlated to the direction of change as determined by the manual linear measurements. The average reduction in lesion volume determined via DTG analysis was 86% as compared to 96% for the manual linear measurements, suggesting that the software more often tended to detect persistence of periapical lesions or areas of incomplete bone fill than did the clinical evaluators. The clinical significance of this refractory lesion volume, however, is unclear and may warrant further investigation.

Analysis of CBCT scans reveals that periapical lesions often assume irregular three-dimensional shapes. The implicit advantage of volumetric measurements over two-dimensional linear measurements is the ability of software algorithms, such as DTG, to accurately approximate the complex geometry of lesions. This geometric accuracy, in turn, may translate to a more meaningful measure of not only post-surgical osseous changes but also the detection of refractory lesions that may alter a clinical treatment plan.

While software-assisted volumetric analysis may provide powerful diagnostic utility, obtaining reproducible and accurate results can be challenging for lesions that are not well-demarcated and confined to trabecular bone. Lesions that perforate the cortical plate or into the maxillary sinus often appear contiguous with those spaces in a CBCT scan. In these circumstances, interpolation of lesion boundaries is complicated by the comparable radiodensities of periapical lesions and communicating anatomic spaces. The grayscale-based algorithm of DTG may also fail to accurately limit the extent of a lesion, instead including anatomic space to the final volumetric output. More generally, volumetric measurements are limited by the overall quality of the source CBCT scan. The presence of scatter, beam hardening,

or other processing artifacts can impact the black/white contrast necessary for DTG to execute its function. Movement of the patient during image acquisition can result in a blurry scan that can also complicate the determination of lesion boundaries.

The challenges that limit an accurate software-assisted volumetric analysis also affect manual linear measurements. Evaluators noted CBCT artifacts in approximately half of the scans within the data set to varying degrees of lesion obfuscation. The role of beam-hardening, in particular, led the oral radiologist to assign several zero-value dimensional measurements in post-operative recall scans. These measured values and their associated parameters can be found in Appendix E.

With the findings of this study confirming the sensitivity of volumetric software to lesion changes, it may be of interest in future studies to establish regular post-surgical follow-ups with CBCT scans. Doing so may allow investigators to plot volumetric change through time and ostensibly establish a projected timeline of post-surgical healing for a cohort of patients. This information would be valuable in the overall assessment of lesion healing and inform clinical decision-making to either continue monitoring patients or pursue an alternative intervention.

In conclusion, this study reports the average reduction in post-apicoectomy lesion volume determined via volumetric software analysis was 86% as compared to 96% for the manual linear measurements of CBCT scans. These two methods of lesion assessment were correlated with one another but more highly correlated in pre-surgical scans than in post-surgical recall scans. Additionally, the use of the B-score to assess post-surgical healing resulted in 88% of lesions being categorized as either healed or showing evidence of healing.

References

1. Figdor D. Apical periodontitis: A very prevalent problem. Oral Surg Oral Med Oral Pathol Oral Radiol Endod. 2002;94(6):651-2.

2. Kakehashi S, Stanley H, Fitzgerald R. The effect of surgical exposures of dental pulps in germ-free and conventional laboratory rats. Oral Surg Oral Med Oral Pathol. 1965;20(3):340-9.

3. Möller A, Fabricius L, Dahlén G, Ohman A, Heyden G. Influence on periapical tissues of indigenous oral bacteria and necrotic pulp tissue in monkeys. Scand J Dent Res. 1981;89(6):475-84.

4. Salehrabi R, Rotstein I. Endodontic treatment outcomes in a large patient population in the USA: An epidemiological study. J Endod. 2004;30(12):846-50.

5. Sundqvist G, Figdor D, Persson S, Sjögren U. Microbiologic analysis of teeth with failed endodontic treatment and the outcome of conservative re-treatment. Oral Surg Oral Med Oral Pathol Oral Radiol Endod. 1998;85(1):86-93.

6. Nair P. New perspectives on radicular cysts: do they heal? Int Endod J. 1998;31:155-60.

7. Kim S. Principles of endodontic microsurgery. Dent Clin North Am 1997;41:481-97.

8. Kim S. Modern Endodontic Surgery Concepts and Practice: A Review. J Endod. 2006;32:601-623.

9. Tsesis I, Rosen E, Taschieri S, Telishevsky S, Ceresoli V, Del Fabbro M. Outcomes of surgical endodontic treatment performed by a modern technique: An updated meta-analysis of the literature. J Endod. 2013;39(3):332-9.

10. Melcher AH. On the repair potential of periodontal tissues. J Periodontol 1976;47:256-60.

11. von Arx T, Jensen S, Hanni S. Clinical and radiographic assessment of various predictors for healing outcome 1 year after periapical surgery. J Endod 2007;33:123-8.

12. Caliskan M, Tekin U, Kaval M, Solmaz M. The outcome of apical microsurgery using MTA as the root-end filling material: 2- to 6-year follow-up study. Int Endod J 2016;49:245-54.

13. Penarrocha M, Marti E, Garcia B, Gay C. Relationship of periapical lesion radiologic size, apical resection, and retrograde filling with the prognosis of periapical surgery. J Oral Maxillofac Surg 2007;65:1526-9.

14. Shinbori N, Grama AM, Patel Y, et al. Clinical outcome of endodontic microsurgery that uses EndoSequence BC root repair material as the root-end filling material. J Endo 2015;41:607-12.

15. Villa-Machado P, Botero-Ramirez X, Tobon-Arroyave S. Retrospective follow-up assessment of prognostic variables associated with the outcome of periradicular surgery. Int Endod J 2013;46:1063-76.

16. Bender IB. Factors influencing the radiographic appearance of bony lesions. J Endod 1997;23:5-14.

17. Roberts J, Drage N, Davies J, Thomas D. Effective dose from cone beam CT examinations in dentistry. Br J Radiol. 2009;82(973):35-40.

18. Low K, Dula K, Burgin W, Arx T. Comparison of periapical radiography radiography and limited cone-beam tomography in posterior maxillary teeth referred for apical surgery. J Endod. 2008;34(5):557-62.

19. Venskutonis T, Plotino G, Tocci L, Gambarini G, Maminskas J, Juodzbalys G. Periapical and endodontic status scale based on periapical bone lesions and endodontic treatment quality evaluation using cone-beam computed tomography. J Endod. 2015;41(2):190-6.

20. Tsai P, Torabinejad M, Rice D, Azevedo B. Accuracy of cone-beam computed tomography and periapical radiography in detecting small periapical lesions. J Endod. 2012;38(7):965-70.

21. Lofthag-Hansen S, Huumonen S, Grondahl K, Grondahl H. Limited cone-beam CT and intraoral radiography for the diagnosis of periapical pathology. Oral Surg Oral Med Oral Pathol Oral Radiol Endod. 2007;103(1):114-9.

22. Ahlowalia M, Patel S, Anwar H, Cama G, Austin R, Wilson R, et al. Accuracy of CBCT for volumetric measurement of simulated periapical lesions. Int Endod J. 2013;46(6):538-46.

23. Patel S, Wilson R, Dawood A, Mannocci F. The detection of periapical pathosis using periapical radiography and cone-beam computed tomography--part 1: pre-operative status. Int Endod J 2012;38:1588-91.

24. Abella F, Patel S, Duran-Sindreu F, et al. Evaluating the periapical status of teeth with irreversible pulpitis by using cone-beam computed tomography scanning and periapical radiographs. J Endod 2012;38:1588-91.

25. von Arx T, Janner S, Hanni S, Bornstein M. Evaluation of new cone-beam computed tomographic criteria for radiographic healing evaluation after apical surgery: Assessment of repeatability and reproducibility. J Endod. 2016;42(2):236-42.

26. Kamburoglu K, Kilic C, Ozen T, Horasan S. Accuracy of chemically created periapical lesion measurements using limited cone beam computed tomorgraphy. Dentomaxillofac Radiol 2010;39:95-9.

27. Liang Y, Jiang L, Gao X, et al. Detection and measurement of artificial periapical lesions by cone-beam computed tomography. Int Endod J 2014;47:332-8.

28. Fu J, Wang H. Reliability of volumetric imaging software for cone-beam computed tomogram scans in the anterior maxilla. Implant Dent 2013;22:182-6.

29. Tanomaru F, Jorge E, Guerreiro-Tanomaru J, et al. Two- and tridimensional analysis of periapical repair after endodontic surgery. Clinical Oral Investig 2015;19:17-25.

30. Cardoso F, Ferreira N, Martino F, Nascimento G, Manhaes Jr L, Rocc M, et al. Correlation between volume of apical periodontitis determined by cone-beam computed tomography analysis and endotoxin levels found in primary root canal infection. J Endod. 2015;41(7):1015-9.

31. Zhang M, Liang Y, Gao X, Jiang L, Sluis L, Wu M. Management of apical periodontitis: Healing of post-treatment periapical lesions present 1 year after endodontic treatment. J Endod. 2015;41(7):1020-5.

32. Kim D, Ku H, Nam T, Yoon T, Lee C, Kim E. Influence of Size and Volume of Periapical Lesions on the Outcome of Endodontic Microsurgery: 3-Dimensional Analysis Using Cone-beam Computed Tomography. J Endod. 2016;42(8):1196-1201.

33. Orstavik D. Time-course and risk analyses of the development and healing of chronic apical periodontitis in man. Int Endod J 1996;29:150-5.

34. Patel S, Wilson R, Dawood A, Foschi F, Mannocci F. The detection of periapical pathosis using digital periapical radiography and cone beam computed tomography - part 2: A 1-year post-treatment follow-up. Int Endod J. 2012 Aug;45(8):711-23.

35. van der Borden WG, Wang X, Wu MK, Shemesh H. Area and 3-dimensional volumetric changes of periapical lesions after root canal treatments. J Endod. 2013 Oct;39(10):1245-9.

36. Liang Y, Jiang L, Jiang L, Chen X, Liu Y, Tian F, et al. Radiographic healing after a root canal treatment performed in single-rooted teeth with and without ultrasonic activation of the irrigant: A randomized controlled trial. J Endod. 2013 Oct;39(10):1218-25.

37. Zhang M, Liang Y, Gao X, Jiang L, van der Sluis L, Wu M. Management of apical periodontitis: Healing of post-treatment periapical lesions present 1 year after endodontic treatment. J Endod. 2015 Jul;41(7):1020-5.

38. Orstavik D, Kerekes K, Eriksen H. The periapical index: A scoring system for radiographic assessment of apical periodontitis. Endod Dent Traumatol. 1986 Feb;2(1):20-34.

39. Estrela C, Bueno M, Azevedo B, Azevedo J, Pecora J. A new periapical index based on cone beam computed tomography. J Endod. 2008 Nov;34(11):1325-31.

40. Goldman M, Pearson A, Darzenta N. Endodontic success--who's reading the radiograph? Oral Surg Oral Med Oral Pathol. 1972 Mar;33(3):432-7.

41. Goldman M, Pearson A, Darzenta N. Reliability of radiographic interpretations. Oral Surg Oral Med Oral Pathol. 1974 Aug;38(2):287-93.

42. Winberg T, Fouad A, Bennett I, Bellingham P, Otis L, Fouad A. A novel approach to the treatment and outcome assessment of apical periodontitis: A double-blind, randomized clinical trial. JOE. 2014 March;40(3):e2.

Appendices

Appendix A: Protocol for Linear Measurement of Lesions

1. Identify the tooth and specific root(s) associated with the lesion in question
2. View the scan using oblique slicing
3. View the scan in 1.2-1.3mm slice thickness

Do the following for the Axial, Coronal, and Sagittal planes:
4. Scan through the entire plane and identify the slice where you feel the lesion has the largest overall area
5. Make a measurement across the lesion (from bone to bone) that represents the largest diameter, or largest measurement of the lesion (note that this measurement can be in any direction across the lesion)*
6. Next, make a measurement at 90 degrees to the initial measurement
7. Record these two measurements
8. Perform these measurements on both the Pre-op & Post-op views, then record your assessment of the change in lesion size over time using the B-score healing index, which is a combination of apical fill (A-score) and cortical plate formation (C-score):

B-score 2: Complete hard tissue ("bony trabecular") fill of former lesion/osteotomy site and formation of an intact cortical plate in its anatomically correct shape
B score 1: Any situation not attributable to B scores 0 or 2
B score 0: Neither hard tissue fill of former lesion/osteotomy site nor formation of cortical plate
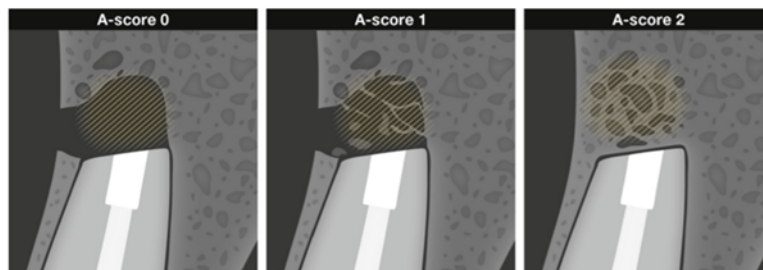
Figure 2. A schematic illustration of the A index (bone formation within the apical area).
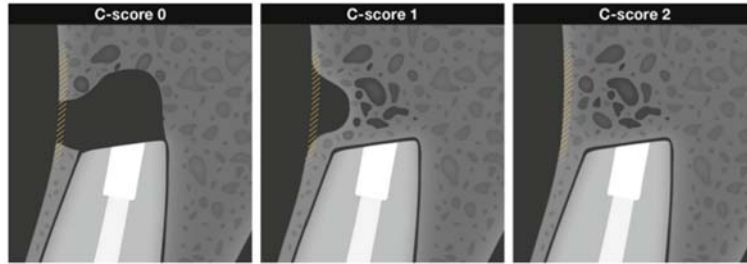
Figure 3. A schematic illustration of the C index (reformation of the cortical plate).

*If the lesion does not have clear bone boundaries (i.e. cortical plate perforation, sinus perforation etc.), then estimate the lesion boundary based upon the bone that can be observed on either side of the defect

Appendix B: DiThreshGUI Protocol

Overall workflow for DiThreshGUI

Install MCR

↓

Run Analysis

↓

Inspect Shape

↓

Organize results

DiThreshGUI is a simple tool for computing the 3d volume of bone lesions or other shapes that have irregular boundaries. This documentation explains how to use it.

Technical inquiries and feature requests:
Anthony Fouad
afouad@seas.upenn.edu (preferred)
anthony.fouad@gmail.com
215-839-9647

Please feel free to ask!

Back to main

Install MCR   1 of 1

DiThreshGUI_2015b requires that you download and install the **Matlab Compiler Runtime R2015b**. MCR is available here:

http://www.mathworks.com/products/compiler/mcr/index.html

MCR is **free** and does not require a Matlab License.
Please select the version that matches your computer system.

MATLAB Compiler

Overview | Features | Videos | Webinars | Related Products | What's New | Product Trial

Note: you can find this information in the `readme.txt` file that accompanies the application or component.

Release (MATLAB Runtime Version#)	Windows	Linux	Mac
R2015b (9.0)	32-bit / 64-bit	64-bit	Intel 64-bit

Alternately, the DTG source code can be run from within Matlab.

43

Run analysis

1. Double click on **DiThreshGUI_2015b**.

2. Click **XY Dicom** to load a stack of dicom images*,**.

3. In the popup window, navigate to your DICOM images. Select **ALL** of them, and press **open**.

* DiThreshGUI will offer to save the 3D stack after it puts together all slices. This stack can be used instead of the dicoms if you click **XYZ mat** next time you run the program.

** All button in DiThreshGUI turn **Red** while they are processing and **Green** when they are done. If a button remains red, it has crashed and you will not be able to continue your analysis. Please contact Anthony.

Run analysis

4. The **Slice** slider bar turns **Yellow**. This indicates it is ready to be used next.

   Navigate through the axial slices until you find the lesion. When ready, click **Select 2 ROIs**.
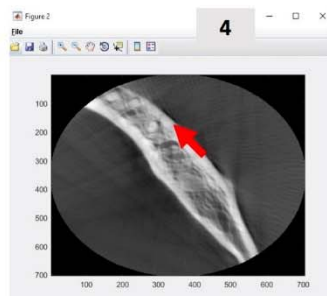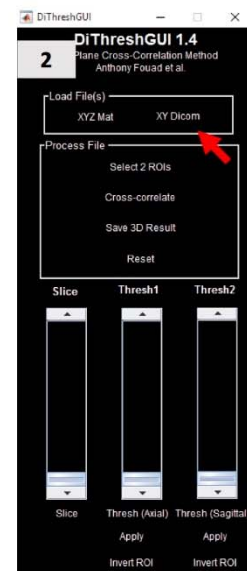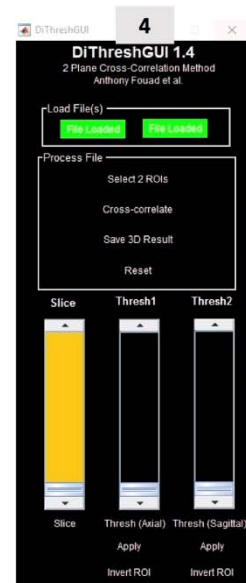
Run analysis

5. Use the polygon tool to draw a subjective boundary around the lesion in the axial plane:

- Click to add a new point
- Click on the first point to close the shape.
- **OR**, double click to force close the shape.
- When finished, **double click** in the center of the shape to exit.

The boundary need not be precise. It is refined by thresholding later. When you preview your 3D results later, you will be able to tell whether the boundary you drew was suitable.
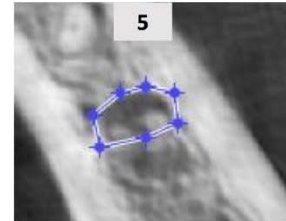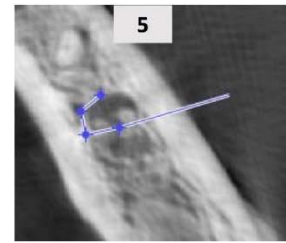
Run analysis

6. A new pop up shows a sagittal slice that passes through the shape you drew in step 5. Again, draw a boundary around your lesion in the sagittal plane. Again, double click to complete*.

7. After a few seconds, Select 2 ROIs turns **Green** to indicate completion and the **Thresh1** slider turns **Yellow**, advising you to use it next.

* DiThreshGUI may crash if the boundary you draw in the sagittal plane does not intersect the boundary you drew in the axial plane. DTG does not currently check for this error – it relies on the user to select the same lesion in both views.
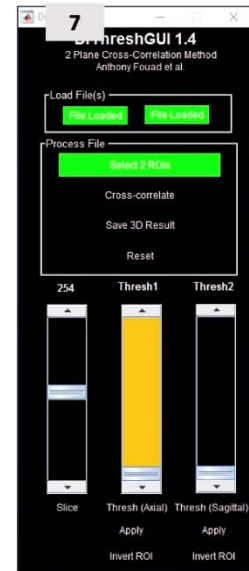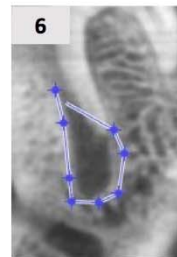
Run analysis

8. Use the **Thresh1** slider to select an appropriate threshold for the lesion*.

9. When satisfied, click **Apply** and then **Invert ROI**.

10. Now, Repeat 6 and 7 with **Thresh2** in the sagittal plane.
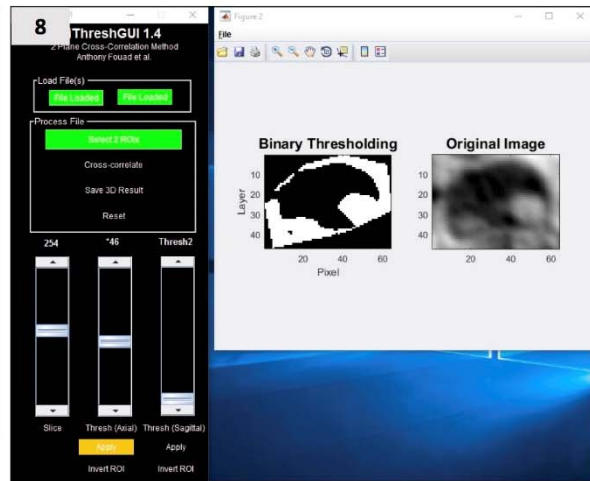
* If needed, you may record the specific threshold and use the same one later (46 in this case)

Run analysis

11. When both thresholds are set, the **Cross-Correlate** button turns **Yellow**, advising you to click it.

12. In the popup window, you can select from 3 display options. Click any combination of these and press **OK*,****.
    A – 3D object
    B – Max Diameters
    C – Max Areas
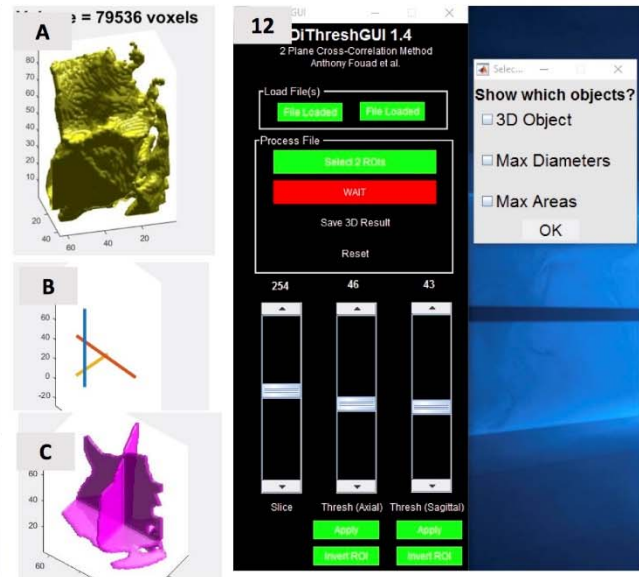
* You can click Cross-Correlate again to try a different graphical representation.
** The rotation tool on the pop up window is useful for adjusting the 3D object's orientation.

Run analysis

How does this work?

The axial threshold your selected is applied to all frames in the axial direction (blue object at right).

The sagittal threshold you selected is applied to all slices in the sagittal direction.

The intersection of these two objects is the lesion.

This algorithm is substantially similar to **Metska et al (2013), JOE, Volumetric Changes in Apical…**, but was developed independently and does not require AMIRA.
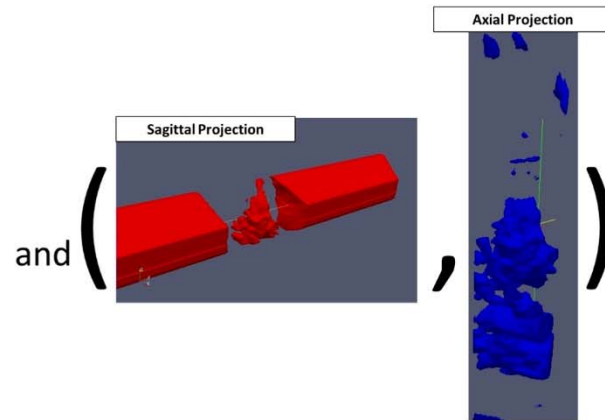
Run analysis

13. Regardless of which 3D view you choose to preview, you can click **Save 3D result** to save all of the information to disk. Type in the patient ID (B#), Tooth #, and Root position (e.g. Mesial) and click **OK**.

14. A .mat file containing all of this information is saved to the same directory as the 3D image you loaded. You can convert this file to an excel file using the **Organize Results** section later.
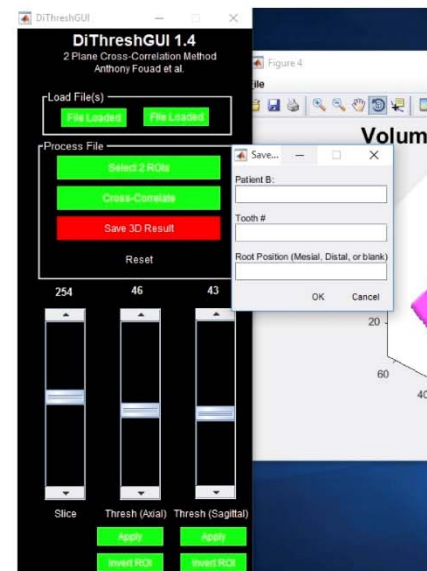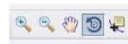
Inspect shape

- Be sure that the 3D shape faithfully represents what you consider to be lesion. In particular, large flat faces (**arrow**) indicate that your shape was cut off by the region(s) of interest you drew. If this is not desired, you can try again with a larger ROI by pressing the **Reset** button.

- In general, the region selection strategy and threshold levels will substantially impact the resulting shape and its reported volume. You should be careful to standardize the thresholds used and train the user on training data before evaluating experimental subjects.

Volume = 79536 voxels
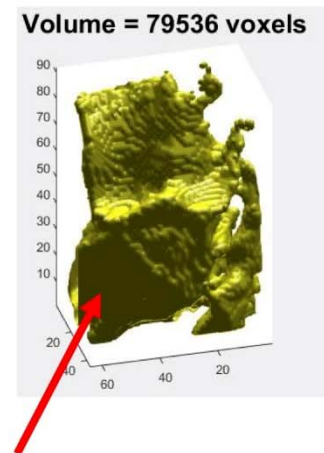
Organize Results

- After completing several 3D analyses, you will have a collection of files with format:

  DTG_B#_tooth#pos.mat

- These files can be collected together into an excel spreadsheet that contains volumetric, diameter and area information using the separate standalone **DTG_reader_2015b**

- Run this application by double clicking on it.

- Click on **Load Files**, and then select ALL of the DiThreshGUI output results you would like to organize.

DTG_reader

DiThreshGUI - READER

0 Files Loaded

Load Files

Produce Spreadsheet

Reset
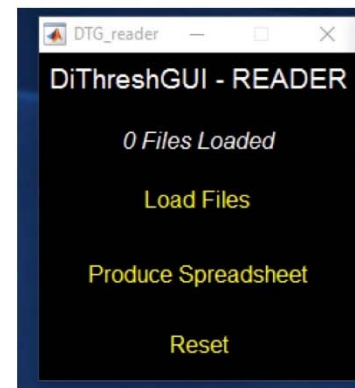
Organize Results

- Click produce spreadsheet when you have all of them. Type a filename.

- A popup tells you where the xlsx was saved (same directory where DTG_reader_2015b is located). This file contains all of the volume, diameter and area information for each file you processed.

	A	B	C	D	E	F	G	H	I	J
1	Measurement:	B01	B05	B07	B07	B07	B77	B88	B88	B12
2	Date of processing	3-Jun-13	22-Sep-15	6-May-13	6-May-13	6-May-13	14-Jul-14	22-Jun-14	22-Jun-14	22-Sep-15
3	Time of processing	09:07.3	18:18.6	48:08.8	50:20.5	43:01.5	37:43.0	16:36.0	27:25.6	21:20.7
4	Axial Threshold	0.61	0.39	0.37	0.37	0.37	0.34	0.4	0.4	0.46
5	Sagittal Threshold	0.61	0.4	0.36	0.36	0.36	0.34	0.41	0.4	0.43
6	Coordinates of lesion (R,C,F):	397,366,403	250,334,241	473,419,280	380,389,273	249,330,252	128,216,285	252,339,234	248,331,234	251,328,254
7	VOL (voxels):	58908	61123	30151	11863	50003	20012	108481	73801	79536
8	Max coronal diameter:	61	33	37	22	30	27	45	35	34
9	Max coronal area:	2084	2678	1089	795	2324	1035	3272	3028	3186
10	Max sagittal diameter:	44	53	46	46	50	37	68	63	64
11	Max sagittal area:	2387	1583	894	392	1363	882	2110	1705	1866
12	Max axial diameter:	64	70	40	32	67	41	79	72	76
13	Max axial area:	1495	1355	1396	564	1190	620	2068	1609	1577
14										

Appendix C: Patients in the Study

Patient	Age	Sex	Date PreOP	Date PostOP	Duration (months)	Teeth
A	72	M	5/4/2012	7/28/2016	50	4
B	75	M	9/19/2012	8/3/2016	47	7
C	70	M	10/1/2013	7/20/2016	33	6
D	67	F	9/15/2014	7/27/2016	22	12
E	46	F	1/15/2014	7/22/2016	30	6, 7, 8, 10, 11, 12
F	76	F	10/1/2013	8/30/2016	34	3, 4
G	74	M	7/17/2012	9/21/2016	50	9
H	55	F	8/13/2014	10/19/2016	26	8
I	84	M	1/5/2015	10/14/2016	21	25
J	60	F	7/28/2015	10/12/2016	15	30
K	78	M	7/15/2011	10/17/2016	63	19
L	56	M	1/28/2015	11/4/2016	22	7
M	56	F	6/7/2013	11/8/2016	41	12
N	66	M	8/27/2013	11/9/2016	39	30
O	68	M	10/18/2011	11/9/2016	61	14
P	64	F	7/14/2015	11/2/2016	16	13
Q	65	F	1/11/2012	12/8/2016	59	30
R	58	F	2/26/2014	12/5/2016	34	30
S	72	M	8/3/2011	11/23/2016	63	7, 9
T	55	M	10/22/2015	11/22/2016	13	27

Appendix D: DTG Volume Measurements (voxels)

Patient	Tooth	PreOP Sagittal Max.	PreOP Coronal Max.	PreOP Axial Max.	PreOP Volume	PostOP Sagittal Max.	PostOP Coronal Max.	PostOP Axial Max.	PostOP Volume
A	4	88	80	67	195096	42	43	37	32417
B	7	48	43	63	61031	56	23	21	10693
C	6	123	93	87	341981	68	35	18	15525
D	12	39	53	59	34575	18	16	7	806
E	6	35	31	36	15923	0	0	0	0
E	7	40	48	33	25154	32	29	13	4980
E	8	51	43	45	35106	25	21	24	4681
E	10	47	52	41	44439	40	47	23	17351
E	11	40	46	53	33557	41	33	19	7618
E	12	57	49	42	43066	37	31	16	8760
F	3	109	134	137	697251	0	0	0	0
F	4	109	134	137	697251	0	0	0	0
G	9	49	52	72	79348	83	62	98	268372
H	8	14	15	7	800	55	63	67	93101
I	25	91	47	55	109877	67	52	39	70304
J	30	67	53	64	86138	85	55	34	75173
K	19	103	84	84	287512	73	61	58	114208
L	7	90	57	46	149718	37	35	21	13902
M	12	42	21	33	13389	92	57	39	99590
N	30	107	100	101	561078	44	24	27	10830
O	14	77	72	58	130287	50	49	29	31325
P	13	81	48	43	63556	45	17	18	4796
Q	30	65	27	26	13252	0	0	0	0
R	30	81	42	58	80702	28	32	14	6072
S	7	86	74	63	188489	50	41	100	68189
S	9	62	41	52	58589	0	0	0	0
T	27	136	70	82	367238	91	33	27	17458

Appendix E: Linear Measurements (mm)

		PreOP						PostOP					
		Sagittal		Coronal		Axial		Sagittal		Coronal		Axial	
Patient	Tooth	Max.	Min.	Max.	Min.	Max.	Min.	Max.	Min.	Max.	Min.	Max.	Min.	B score
Examiner=								One						
A	4	4.8	3.6	5.1	3.5	6.4	5.3	1.6	0.8	1.9	1.3	0.0	0.0	1
B	7	3.5	3.2	2.4	1.8	1.2	1.2	1.4	1.0	3.3	1.6	0.0	0.0	1
C	6	7.2	6.5	6.6	5.7	7.5	6.0	0.0	0.0	1.3	0.7	0.0	0.0	2
D	12	3.3	5.4	3.0	6.7	4.0	3.4	4.2	3.7	6.2	3.4	4.5	3.9	0
E	6	3.0	4.6	1.8	3.9	1.4	1.7	0.0	0.0	0.0	0.0	0.0	0.0	2
E	7	2.8	1.3	3.7	1.6	2.4	3.7	3.0	0.5	2.6	0.5	1.0	3.3	1
E	8	2.4	2.4	3.6	3.0	3.6	1.8	0.0	0.0	0.0	0.0	0.0	0.0	2
E	10	4.1	1.6	3.8	3.7	3.7	3.2	4.9	0.7	1.6	1.0	1.5	2.8	1
E	11	3.2	5.6	2.4	3.3	3.4	3.3	0.0	0.0	0.0	0.0	0.0	0.0	2
E	12	3.4	2.0	3.4	3.6	4.5	3.0	0.0	0.0	0.0	0.0	0.0	0.0	2
F	3	9.9	11.7	8.2	11.3	7.4	10.6	2.2	6.1	3.7	4.9	3.6	3.2	1
F	4	10.1	11.1	5.8	12.1	6.5	9.6	1.9	2.3	1.6	4.2	0.9	2.3	1
G	9	3.0	7.0	2.5	8.7	1.5	2.6	2.8	5.2	2.0	8.0	3.1	4.3	0
H	8	0.0	0.0	0.8	0.7	1.4	0.6	3.6	3.1	2.8	3.7	2.0	3.1	1
I	25	3.6	3.7	5.6	3.1	6.1	3.2	3.9	2.0	3.4	2.0	3.1	4.0	0
J	30	3.1	3.3	4.2	1.7	3.1	4.7	1.4	2.2	3.8	1.1	1.3	4.4	1
K	19	5.8	7.5	6.0	9.0	6.5	5.6	4.2	4.0	4.1	3.0	4.5	3.5	1
L	7	4.8	2.9	4.3	3.7	4.8	3.4	0.0	0.0	0.0	0.0	0.0	0.0	1
M	12	1.8	2.1	1.4	1.4	1.7	0.9	5.2	3.5	2.4	1.4	2.1	2.1	0
N	30	7.6	7.4	7.0	7.6	7.0	7.8	0.0	0.0	0.0	0.0	0.0	0.0	2
O	14	4.6	3.3	5.6	3.5	5.2	3.8	0.8	3.1	3.3	1.0	2.0	1.2	1
P	13	2.0	5.8	4.8	5.4	4.1	3.2	0.0	0.0	0.0	0.0	0.0	0.0	2
Q	30	3.1	1.3	2.3	2.6	0.0	0.0	0.0	0.0	0.0	0.0	0.0	0.0	2
R	30	5.4	6.5	3.1	3.7	5.8	5.1	0.0	0.0	0.0	0.0	0.0	0.0	2
S	7	4.9	11.7	5.1	9.2	5.8	5.3	1.8	0.7	1.6	3.0	1.4	4.2	1
S	9	2.6	7.1	0.0	0.0	5.7	1.5	0.0	0.0	0.0	0.0	0.0	0.0	1
T	27	4.6	1.9	9.9	5.7	8.9	4.6	0.0	0.0	0.0	0.0	0.0	0.0	2

		PreOP						PostOP						
		Sagittal		Coronal		Axial		Sagittal		Coronal		Axial		
Patient	Tooth	Max.	Min.	Max.	Min.	Max.	Min.	Max.	Min.	Max.	Min.	Max.	Min.	B score
Examiner=								Two						
A	4	8.2	7.5	6.0	5.7	7.1	6.3	4.0	2.3	4.5	2.0	4.1	3.0	1
B	7	3.5	2.8	3.7	2.7	3.6	2.7	3.5	2.5	3.5	1.8	0.0	0.0	1
C	6	8.1	7.8	7.5	7.3	8.4	7.1	5.0	4.1	4.6	4.1	5.0	3.9	1
D	12	5.5	3.6	6.7	5.8	5.6	3.6	4.8	4.6	6.7	5.8	4.6	4.3	1
E	6	3.4	2.4	4.3	2.1	3.1	2.3	0.0	0.0	0.0	0.0	0.0	0.0	2
E	7	2.9	2.7	3.5	2.7	0.0	0.0	0.0	0.0	0.0	0.0	0.0	0.0	2
E	8	3.7	2.8	3.6	2.7	4.1	2.6	0.0	0.0	0.0	0.0	0.0	0.0	2
E	10	4.2	3.5	4.5	3.7	4.1	3.7	4.0	1.6	3.5	0.8	0.0	0.0	1
E	11	4.4	3.2	3.8	3.7	3.9	3.2	0.0	0.0	0.0	0.0	0.0	0.0	2
E	12	3.6	3.1	4.6	3.9	2.9	2.7	0.0	0.0	0.0	0.0	0.0	0.0	2
F	3	12.0	10.2	11.2	11.0	10.4	9.3	0.0	0.0	0.0	0.0	0.0	0.0	2
F	4	11.3	10.1	12.3	11.3	10.5	9.5	0.0	0.0	0.0	0.0	0.0	0.0	2
G	9	8.7	5.3	6.6	2.1	4.1	2.8	8.7	5.8	5.8	2.1	4.7	1.3	0
H	8	0.0	0.0	0.0	0.0	0.0	0.0	4.8	3.7	5.2	4.3	4.5	3.6	0
I	25	4.9	4.6	4.5	3.7	4.0	3.5	5.8	4.1	4.6	4.4	0.0	0.0	1
J	30	3.7	3.0	5.2	4.3	4.3	3.1	2.4	2.1	5.1	1.9	4.1	2.7	2
K	19	7.1	5.9	7.3	4.6	8.1	5.1	5.7	5.2	4.9	4.1	5.1	4.0	2
L	7	5.2	4.0	5.0	4.7	5.1	3.9	0.0	0.0	0.0	0.0	0.0	0.0	1
M	12	2.9	2.2	2.4	1.7	2.0	1.7	5.1	4.7	3.0	1.7	0.0	0.0	0
N	30	8.1	8.0	8.2	6.9	7.8	7.1	0.0	0.0	0.0	0.0	0.0	0.0	2
O	14	4.5	4.1	5.3	4.6	6.8	3.9	0.0	0.0	0.0	0.0	0.0	0.0	1
P	13	6.5	4.1	6.1	5.3	4.7	3.2	0.0	0.0	0.0	0.0	0.0	0.0	2
Q	30	0.0	0.0	0.0	0.0	0.0	0.0	0.0	0.0	0.0	0.0	0.0	0.0	1
R	30	7.6	6.0	7.0	6.0	5.7	5.3	0.0	0.0	0.0	0.0	0.0	0.0	2
S	7	11.1	8.9	11.1	6.5	5.6	5.5	0.0	0.0	0.0	0.0	0.0	0.0	2
S	9	0.0	0.0	0.0	0.0	0.0	0.0	0.0	0.0	0.0	0.0	0.0	0.0	1
T	27	9.5	7.2	5.5	5.0	7.6	4.5	2.9	2.6	5.2	3.1	0.0	0.0	1

Vita

Dr. Eshwar Arasu was born on September 10, 1989 in Pondicherry, India and is a United States citizen. He received a Bachelor of Science in Engineering in Biomedical Engineering from the University of Michigan in 2011 before attending the Harvard School of Dental Medicine where he earned a Doctor of Dental Medicine in 2015. He is a member of the American Dental Association and the American Association of Endodontists. Dr. Arasu will graduate from Virginia Commonwealth University with a Master of Science in Dentistry and a Certificate in Endodontics.